

1 **MINERALOGICAL AND CHEMICAL CHARACTERIZATION**  
2 **OF LUNAR HIGHLAND SOILS:**  
3 **INSIGHTS INTO THE SPACE WEATHERING**  
4 **OF SOILS ON AIRLESS BODIES**

5  
6 **Lawrence A. Taylor<sup>1</sup>, Carlé Pieters<sup>2</sup>,**  
7 **Allan Patchen<sup>1</sup>, Dong-Hwa S. Taylor<sup>1</sup>,**  
8 **Richard V. Morris<sup>3</sup>, Lindsay P. Keller<sup>3</sup>, and David S. McKay<sup>3</sup>**

9  
10 **<sup>1</sup> Planetary Geosciences Institute**  
11 **Dept. of Earth & Planetary Sciences**  
12 **University of Tennessee**  
13 **Knoxville, TN 37996, ([lataylor@utk.edu](mailto:lataylor@utk.edu))**

14  
15 **<sup>2</sup> Dept. of Geological Sciences**  
16 **Brown University**  
17 **Providence, RI 02912**

18  
19 **<sup>3</sup> Code KR**  
20 **NASA/Johnson Space Center**  
21 **Houston, TX 77058.**

22  
23 **SUBMITTED TO: Journal Of Geophysical Research**

24 **CONTACT: Larry Taylor**

25 **REVISED: 9 August 2009**

26 **Abstract.** With reflectance spectroscopy, one is measuring only properties of the fine-grained  
27 regolith, most affected by space weathering. The Lunar Soil Characterization Consortium has  
28 undertaken the task of coordinated characterization of lunar soils, with respect to their mineralog-  
29 ical and chemical makeup. It is these lunar soils that are being used as “ground-truth” for all air-  
30 less bodies. Modal abundances and chemistries of minerals and glasses in the finest size frac-  
31 tions (20-45, 10-20, and <10  $\mu\text{m}$ ) of four Apollo 14 and six Apollo 16 highland soils have been  
32 determined, as well as their bulk chemistry and  $I_S/\text{FeO}$  values. Bi-directional reflectance mea-  
33 surements (0.3–2.6  $\mu\text{m}$ ) of all samples were performed in the RELAB. A significant fraction of  
34 nanophase  $\text{Fe}^0$  (np- $\text{Fe}^0$ ) appears to reside in agglutinitic glasses. However, as grain size of a soil  
35 decreases, the percentage of total iron present as np- $\text{Fe}^0$  increases significantly, whereas the ag-  
36 glutinitic glass content rises only slightly; this is evidence for a large contribution to the  $I_S/\text{FeO}$   
37 values from the surface-correlated nanophase  $\text{Fe}^0$ , particularly in the <10  $\mu\text{m}$  size fraction. The  
38 compositions of the agglutinitic glasses in these fine fractions of the highland soils are different  
39 from the bulk-chemistry of that size; however, compositional trends of the glasses are not the  
40 same as those observed for mare soils. It is apparent that the glasses in the highland soils contain  
41 chemical components from outside their terrains. It is proposed that the Apollo 16 soils have  
42 been adulterated by the addition of impact-transported soil components from surrounding maria.

43

44

## 45 **1. Introduction**

46 The varied processes of space weathering that occur during soil formation on the Moon are  
47 thought to be similar to those for many other airless bodies (e.g., Phobos, Eros, Mercury) al-  
48 though different in magnitude and cumulative effect. Therefore, the study of these effects within  
49 lunar soils should form the basis for our understanding of the regoliths on other heavenly bodies.  
50 This is a particularly applicable axiom for reflectance spectroscopy of these soils. It has been  
51 repeatedly demonstrated that it is the fine fractions (<45  $\mu\text{m}$ ) that dominate the spectral reflec-  
52 tance signatures of lunar soils [Pieters, 1983, 1993; Pieters et al., 1993; Hapke, 2001]. The 10-20  
53  $\mu\text{m}$  size fraction is the most similar to the overall spectral properties of the bulk soil. However, it  
54 is also the finer-size fractions that concentrate the major products of space weathering, e.g., na-  
55 nophase metallic iron (np- $\text{Fe}^0$ ), that affect the overall continuum and strength of absorption fea-

56 tures of the observed spectra.

57 Using the Apollo and Luna lunar soils to document the products of space weathering, we  
58 have studied a selected suite of the Apollo 14 and 16 highland soils (**Table 1**). This study is a  
59 continuation to our characterization of the mineralogical and glassy components of the fine frac-  
60 tions of lunar mare soils [e.g., Taylor et al., 2001a, b; Pieters et al., 2000, 2001], especially the  
61 complicated agglutinitic glass [Basu et al., 1996; Basu and Molinaroli, 2001;]. Specific soils  
62 were chosen for their representation of diverse degrees of maturation. These Apollo highland  
63 soils may represent a large portion of the nearside of the Moon. Many systematics of the pro-  
64 gression of soil properties with decreasing grain size are similar to those of mare soils, which ap-  
65 peared to support the Fusion-of-the-Finest Fraction model [Papike et al., 1982] for lunar soil  
66 formation. However, the relationships of the bulk composition of the size fractions for the Apol-  
67 lo 14 and 16 soils to that of the composition of agglutinitic glass are quite different from those  
68 for mare soils and appear to be in an opposite sense. This may necessitate modifications to the  
69 soil formation paradigm, and was first addressed by Pieters and Taylor [2003a].

### 70 **1.1. Lunar Soil Characterization Consortium**

71 In order to document the space weathering effects on lunar spectra, the Lunar Soil Characte-  
72 rization Consortium (LSCC) was established [Taylor et al., 1999; 2001b] for the collaborative  
73 study of lunar soils. This group of lunar soil scientists brings different expertise and instrumental  
74 techniques related to the quantification of space-weathering effects and the deciphering of these  
75 effects in reflectance spectra. The members of this LSC Consortium are D.S. McKay {size sepa-  
76 ration}, R.V. Morris {FMR}, L.P. Keller {TEM/SEM}, C.M. Pieters {Spectral Reflectance}, and  
77 L.A. Taylor {bulk chemistry; modal characterization/mineral chemistry}.

### 78 **1.2. Suite of Lunar Highland Soils**

79 In a logical continuation of our soil characterization studies for mare soils, we have selected a  
80 suite of lunar highland soils to represent the diversity in soil maturities, using the concept of  
81  $I_{\text{q}}/\text{FeO}$  values from Morris [1976]. These soils are listed in Table 1. “Pristine” samples of each  
82 of them were allocated by the Curation and Planning Team for Extra-Terrestrial Materials  
83 (CAPTEM), and the curatorial staff at Johnson Space Center efficiently handled the necessary  
84 allocations. The actual sample handling logistics and allocations are presented in Figure 1 of

85 Taylor et al. [2001a].

## 86 **2. Methodology**

### 87 **2.1. Size Separation**

88 Four Apollo 14 and six Apollo 16 highland soils were sieved in the laboratory of D.S.  
89 McKay at Johnson Space Center. Triply-distilled water was used through out the process. At  
90 first, the lunar sample allocation of the <1 mm size portion of each pristine soil was sieved to ob-  
91 tain a <45  $\mu\text{m}$  size fraction. A split of this <45  $\mu\text{m}$  fraction was then sieved into the three size  
92 ranges: 20-45  $\mu\text{m}$ , 10-20  $\mu\text{m}$ , and <10  $\mu\text{m}$ . Great care was taken to assure the size fractions retain  
93 their natural soil properties, especially grain coatings. According to the same distribution plan as  
94 utilized for the mare soils [Taylor et al., 2001b], samples of each of the size splits were taken and  
95 distributed to members of the LSCC for their specific analysis.

### 96 **2.2. Bulk-Sample Chemical Analyses**

97 Major-element chemistry was determined on portions of each size fraction. The fused-  
98 bead technique was used for preparation of the samples for electron microprobe analyses. In a  
99 stream of dry nitrogen gas, approximately 5 mg of representative sample was fused on a Mo-strip  
100 heater. The samples were heated to a melt, held for 20-30 sec, and quenched by rapidly reducing  
101 the heat input (i.e., turning off the current). The resulting glasses were mounted in a multi-holed  
102 plastic disk, impregnated with epoxy, polished, coated with carbon, and subjected to at least 10  
103 electron microprobe analyses per glass, using a 20  $\mu\text{m}$  beam size, 15 Kv potential, and 20 nA  
104 beam current on the Cameca SX-50 EMP at the University of Tennessee.

### 105 **2.3. Modal Analyses by Electron Microprobe**

106 Detailed petrographic properties of lunar highland soils, particularly the finer fractions, are  
107 poorly known. With these fine-grain sizes (i.e., <45  $\mu\text{m}$ ), normal optical-microscopic techniques,  
108 that are typically used are not efficient. Therefore, modern techniques are required to character-  
109 ize soil compositions and mineral modes with the accuracy and precision needed for spectroscop-  
110 ic modeling. The polished grain mounts prepared by the Curatorial Staff at Johnson Space Cen-  
111 ter formed the basis for all modal and phase characterization. Using the technique presented by  
112 Taylor et al. [1996], accurate modal analyses were performed with an Oxford Instrument Energy

113 Dispersive Spectrometer Unit (EDS) on a Cameca SX-50 electron microprobe at the University  
114 of Tennessee. Through use of Oxford Instruments *FeatureScan* software, it was possible to rea-  
115 dily determine the modal proportions of minerals and glasses in thousands of fine particles in the  
116 20-45  $\mu\text{m}$ , 10-20  $\mu\text{m}$ , and  $<10 \mu\text{m}$  size fractions of the lunar soils. This is based upon gathering  
117 energy dispersive (EDS) chemical data from 150,000-200,000 points on the phases (not epoxy)  
118 in each grain mount, thereby classifying the minerals by their chemistry. Additional programs  
119 allowed for the determination of the average chemical composition of each mineral and glass  
120 phase. The phase compositional data, as well as all our soil characterization data for both the  
121 mare and the highland soils studied by the LSCC are accessible at  
122 <http://web.utk.edu/~pgi/data.html>.

#### 123 **2.4. Difficulties in Modal Analyses of Minerals and Glasses in Highland Soils**

124 The first studies of the LSCC were performed with mare soils [Taylor et al., 2001a, b], and  
125 mare soils were chosen to start our characterization because they contain minerals and glasses  
126 that have vastly contrasting chemistries – e.g., pyroxene versus plagioclase versus agglutinitic  
127 glass – thereby making their identification by chemistry relatively easy. It was anticipated that  
128 applications of our mare-based, X-ray digital-imaging analysis scheme to highland soils would be  
129 considerably more difficult and time-consuming than for the mare soils. This is largely due to  
130 the limited compositional range of highland soils, each with a bulk composition that approx-  
131 imates plagioclase feldspar with only minor mafic components (e.g., ~5 wt% FeO). These sever-  
132 al considerations needed to be made in order to make more effective the application of our tech-  
133 niques to highland soils.

134 The composition of the minerals and glasses in the three size fractions of the four Apollo 14  
135 and six Apollo 16 soils (Table 1) were determined by the extensive analyses of each phase. The  
136 agglutinitic glass was especially placed in close scrutiny. Inasmuch as the composition of the ag-  
137 glutinitic glass in highland soils is not far removed from that of the highland bulk soil, and the  
138 bulk soil is near that of pure plagioclase, this glass closely mimics plagioclase. Therefore, expe-  
139 riments were conducted with the electron microprobe and the EDS unit in order to consider the  
140 several key parameters that determine the precision of the EDS X-ray analyses [Taylor et al.,  
141 2001c; 2002; 2003]. For example, it was been observed that 20 kV excitation is better than the

142 15 kV typically used by most EMP users [Taylor et al., 1996].

143 For the highland soils, a digital map of the entire section of the grain mount is first made,  
144 and many agglutinates, displaying vesicular texture, as well as other phases, are optically identi-  
145 fied by reflected light microscopy. The initial examination with the EMP consists of wave-  
146 length-dispersive spectral (WDS) EMP determinations of the compositional limits of all the opti-  
147 cally identified minerals and glasses from direct analyses of ~1000-3000 phases, in particular the  
148 agglutinitic glasses. With a given soil, it is necessary to perform such initial characterization, for  
149 even subtle differences in chemistry can change the “chemical windows” for a mineral or glass.  
150 In particular, the agglutinitic glasses are all alumina-rich, but the agglutinitic glass, and the minor  
151 amount of non-agglutinitic impact glass, can be distinguished from plagioclase (including maske-  
152 lynite) by their FeO and MgO contents. As demonstrated by McGee [1993], all lunar highland  
153 plagioclase contains <0.5 wt% FeO and <0.5 wt% MgO. We verified this for the identified ag-  
154 glutinitic and impact glasses. These glasses then formed the compositional basis for our EDS  
155 modal analyses.

156 In this study, non-agglutinitic, impact-produced glasses are also reported as agglutinitic glass,  
157 since the compositions from our analyses appear similar and because most of the impact-  
158 produced glasses in the fine-grain sizes examined in this study contain np-Fe<sup>0</sup>. In the modal val-  
159 ues for agglutinitic glass, we estimate that the other non-agglutinitic, impact glasses usually con-  
160 sist of <10% of the glass present. There is no doubt that some small amount of “non-agglutinitic  
161 (i.e., impact) glasses” might have been included, particularly in the finest grain size.

## 162 **2.5. Ferromagnetic Resonance (FMR) Analyses**

163 The detection and analyses of the abundances of single-domain np-Fe<sup>0</sup> were determined by  
164 Ferromagnetic Resonance (FMR) measurements performed in the Magnetism Lab of R.V. Mor-  
165 ris, at Johnson Space Center. It has been in this laboratory that virtually all the FMR measure-  
166 ments on lunar samples have been made since 1972, ensuring consistency, accuracy, and preci-  
167 sion.

## 168 **3. Modal Analyses of Minerals and Glasses**

169 The modal abundances of 12 different minerals and glasses were determined on polished

170 grain mounts of each of the 30 size splits (10 soils X 3 sizes). This was performed utilizing the  
171 X-ray digital imaging technique outlined by Taylor et al. [1996], with several modifications de-  
172 tailed above. The modal data for the major phases in the Apollo 14 and 16 soils are given in Ta-  
173 ble 2 and graphically shown in Figure 1. The pyroxene values are for total pyroxene, calculated  
174 by combining abundances of the four (4) different pyroxene compositions that were determined.  
175 The actual breakdown of these total-pyroxene abundances is given in Table 3. It should be no-  
176 ticed that a designation has been made for a “K-phase”, which is for the “KREEPY” phases (e.g.,  
177 K-rich feldspar; K-rich glasses) typically associated with the Apollo 14 soils. The compositions  
178 of the minerals and agglutinitic glass in the size fractions of these Apollo soil are given in Table  
179 4.

180 As shown by comparison of different soils in Figure 1, there is an overall increase in the ab-  
181 undance of agglutinitic glass as the soils mature, from low to high  $I_S/FeO$  values. This correlates  
182 with the general decrease in the amounts of the minerals and is to be expected, since the longer  
183 the exposure of soil on the surface of the Moon, the greater the effects of micro-meteorite gar-  
184 dening and general space weathering (Taylor and McKay, 1992). This extended presence at the  
185 lunar surface results in an increase in the melted products (i.e., agglutinates, agglutinitic glass,  
186 and vapor-deposited patinas), due to the impacting processes.

187 Within a given soil, a similar scheme is apparent from larger to finer size fractions. With  
188 decrease in grain size, the abundances of the agglutinitic glasses increase (with the exception of  
189 the  $<10\ \mu\text{m}$  fraction of 14141-5.7). Although there is also a tendency for the plagioclase to  
190 slightly increase in the finer fractions, there are distinct decreases in pyroxene and olivine with  
191 decreasing grain size. Therefore, the ferro-magnesian minerals decrease proportionately, while  
192 the plagioclase abundances stay constant or increase slightly. These trends are also apparent with  
193 the bulk chemistry of the various size fractions, as presented below.

194 The designation of ilmenite in the modes includes minor amounts of Ti-Cr-rich spinels  
195 ( $<1\%$ ). Although low in abundance (i.e.,  $<2\%$ ), ilmenite in the Apollo 14 soils, in particular,  
196 shows a general slight increase with decreasing grain size (Table 2), contrary to that in mare soils  
197 [Taylor et al., 2001a, b]. These observations for the Apollo 14 and 16 soils, some of which were  
198 also seen with the mare soils, are addressed by Pieters and Taylor [Pieters and Taylor, 2002,  
199 2003a, b].

200

## 201 **4. Soil Chemistry**

202 Several systematic changes can be readily observed in Figure 2 and Table 4 with respect to  
203 the bulk chemistry of each of the size fractions of the highland soils. The composition of a lunar  
204 highland soil systematically changes as a function of grain size. With a decrease in grain size,  
205 the soils: a) increase in plagioclase components (e.g., CaO, Al<sub>2</sub>O<sub>3</sub>) and b) decrease in olivine and  
206 pyroxene components (e.g., FeO, MgO). It appears that similar soil-formational processes may  
207 occur in the highlands as in the maria. That is, the finest fractions of both the mare and Apollo  
208 14 and 16 soils become enriched in plagioclase components. This observation for the mare soils  
209 originally led us to conclude [Taylor et al., 2001a, b] that the data appeared to support the Fusion  
210 –of-the-Finest Fraction model of agglutinate formation by Papike et al. [1982].

211 There is a systematic and predictable increase of I<sub>S</sub>/FeO with decreasing grain size, a result  
212 of the increased presence of single-domain, np-Fe<sup>0</sup>, as originally observed by Morris [1978]. Al-  
213 though the absolute amount of FeO decreases in the finer fractions, the percentage of this iron  
214 that is present in the metallic Fe<sup>0</sup> state as np-Fe<sup>0</sup> increases significantly. This is indicated by the  
215 large increase in I<sub>S</sub>/FeO values with decreasing grain size (Fig. 2), not proportionate to the much  
216 smaller increases in the abundances of agglutinitic glass, similar to in the mare soils [Taylor et  
217 al., 2001b].

## 218 **5. Mineral and Glass Chemistry**

219 As part of our extensive characterization of the fine-grain sizes of highland soils, we have  
220 determined the average compositions of each of the several phases in the three size fractions. In  
221 Table 5, we have presented these compositions for the 20-45 and 10-20 μm fractions of the soils.  
222 The precisions associated with these averages are quite large, and we have included the 2σ preci-  
223 sions for the agglutinitic glasses, which are by far the largest of all. This illustrates the general  
224 findings of several studies of agglutinitic glass in that the compositions actually range between  
225 pure plagioclase and that of the mafic minerals, olivine and pyroxene (e.g., Hu and Taylor, 1977).  
226 As shown in Figure 3, comparison of the average composition of the agglutinitic glass in the dif-  
227 ferent size fractions of a given soil are approximately constant, particularly when the precisions  
228 are taken into consideration.

229 With the mare soils (Taylor et al., 2001b), the compositions of the 20-45, 10-20, and <10 μm



230 fractions became progressively similar to the agglutinitic glass, with the glass being higher in  
231 plagioclase components (i.e., CaO, Al<sub>2</sub>O<sub>3</sub>). However, the agglutinitic glass for the highland soils  
232 does not demonstrate such a well-defined trend. In fact, the progression from coarse to fine frac-  
233 tions has the composition of the size fractions becoming more plagioclase rich, but the agglutinitic  
234 glass becomes enriched slightly but distinctly in the mafic components (e.g., FeO, MgO), as  
235 illustrated in Figure 3. Although the standard deviation of the average agglutinitic glass compo-  
236 sitions is large, the data for highland soils are systematic. These unexpected results, in contrast  
237 to those for the mare soils, would appear to indicate that either the F<sup>3</sup> model does not adequately  
238 explain the formation of the highland soils or some other process, such as an addition of a mare  
239 component, has been operative.

### 240 **5.1 Chemistry of Highland Agglutinates**

241 A perplexing aspect of the chemical data for the highland soils is present when comparing  
242 TiO<sub>2</sub> contents of the size separates compared to that of the agglutinitic glass, similar to that for  
243 Ti-rich soils [Taylor et al., 2001a, b). Although ilmenite is present in the finest fractions of mare  
244 soils in proportions correlated to the type of basalt, the agglutinitic glass was observed to be dep-  
245 leted in TiO<sub>2</sub> by more than a factor of two; strongly suggesting ilmenite did not enter the glass in  
246 proportion to its abundance in basaltic soils [Pieters et al., 2002].

247 However, the opposite occurs with highland soils. As shown dramatically in Figure 4, the  
248 TiO<sub>2</sub> contents of the Apollo 16 agglutinates are distinctly enriched compared to the chemistry of  
249 the size-fractions of the soils. In fact, it is not only the TiO<sub>2</sub> contents. The chemistry of the high-  
250 land agglutinates in Figure 4, as taken from Table 5, shows that for the Apollo 16 soils, the ag-  
251 glutinitic glass has a distinct enrichment in TiO<sub>2</sub>, Cr<sub>2</sub>O<sub>3</sub>, MgO, FeO, and K<sub>2</sub>O, compared to the  
252 bulk chemistry of each size fraction. This strongly supports the paradigm that there has been  
253 large-scale mixing between mare and highlands [Pieters and Taylor, 2003a]. But, it was the glass  
254 component of the maria that appears to have been selectively added to the Apollo 16 site. This  
255 may well have masked the possible Fusion-of-the-Finest Fraction effects.

### 256 **6. Visible to Near-infrared Spectroscopy of Highland Soils**

257 Bidirectional reflectance spectra for the bulk soil and size separates are shown for all Apollo  
258 14 and 16 soils in Figure 5. The presence of np-Fe<sup>0</sup> both in the agglutinitic glass and on the sur-  
259 faces of grains greatly affects the optical properties of materials exposed to the space environ-

260 ment (e.g., Hapke, 2001; Noble et al., 2001, 2007). The least weathered soils (14141 and 61221)  
261 exhibit the most prominent absorption bands diagnostic of the mafic minerals present, largely  
262 low-calcium pyroxene. The finest fraction not only contains the lowest abundance of mafic min-  
263 erals (Table 2), but it also contains the highest proportion of np-Fe<sup>0</sup> (Fig 2). Diagnostic absorp-  
264 tions are weak or nonexistent in the finest fraction. Similarly, coarse-grained separates contain  
265 fewer agglutinates, proportionately greater mafic minerals, and have smaller surface to volume  
266 ratios than the finer grained separates. Coarse-grained separates thus always exhibit more promi-  
267 nent absorption bands than fine-grained separates from the same soil sample.

268 There is considerable variation of the composition of different size fractions for the same soil  
269 (e.g., Fig 2), and it is difficult to reliably quantify the bulk mineralogy for a given soil. Most ab-  
270 undance analyses are performed on limited amounts of size fraction, and these data must be used  
271 with caution as representations of a soil as a whole. Nevertheless, based on the close similarity  
272 of spectra for the 10-20  $\mu\text{m}$  size fraction with the bulk soil seen across Figure 5, this size fraction  
273 appears to capture a good balance of diverse competing soil processes. We thus recommend the  
274 10-20  $\mu\text{m}$  size fraction be used as a proxy for the bulk when measurements are impractical or  
275 impossible for the bulk soil.

276

## 277 **7. Discussion**

278 The chemistries of the bulk-soil size fractions of the highland soils have similar trends as  
279 compared to those of the mare soils. With decreasing grain size, the soil compositions become  
280 enriched in plagioclase (CaO, Al<sub>2</sub>O<sub>3</sub>) and depleted in mafic components (FeO, MgO). The same  
281 general trends also exist for both the mare and highland soils with respect to the modal mineral  
282 and glass abundances. As with the mare soils, the large increases in the I<sub>S</sub>/FeO values, with de-  
283 crease in grain size, are not proportional to the more minor increases in abundances of the agglu-  
284 tinitic glasses. This large increase in I<sub>S</sub>/FeO is attributed to np-Fe<sup>0</sup> that accumulates on the sur-  
285 faces of the soil particles, as discussed for mare soils [Hapke, 2001; Noble et al., 2001; Pieters et  
286 al., 2000, 2001; Taylor et al., 2001a, b; Keller and McKay, 1997; Keller et al., 2000; Wentworth  
287 et al, 1999].

288 In addition, the unexpected enrichment of the highland agglutinitic glass in mafic components,  
289 compared to the compositions of the bulk-soil fractions for Apollo 16 highland soils, has necessi-

290 tated reconsideration of operative processes for the evolution of lunar soils, previously addressed  
291 by Pieters and Taylor [2003a]. In particular, the role of selective comminution, lateral mixing,  
292 and preferential melting of local components are all clearly important. The suspected large scale  
293 mixing between mare and highlands may be real; however, it is the glass chemistry of the mare  
294 that is preferentially added to the highlands (i.e.,  $\text{TiO}_2$ ,  $\text{Cr}_2\text{O}_3$ ,  $\text{MgO}$ ,  $\text{FeO}$ , and  $\text{K}_2\text{O}$ ). The rego-  
295 lith differential melting sequence, for both highland and mare soils, would appear to be: glass >  
296 plagioclase > pyroxene >> ilmenite. Furthermore, it would seem that lunar mafic-rich glass is  
297 more likely to melt than Al-rich glass, since mare soils tend to accumulate a higher overall abun-  
298 dance of agglutinitic glass than highland soils [Taylor et al., 2001a, b, 2003]. Couple this with  
299 the fact that the finer portions of the soil, the ones with dominant agglutinitic glass, are ballisti-  
300 cally transported greater distances by impact processes, perhaps enhanced by electrostatic levita-  
301 tion [Farrell et al, 2008]. With these considerations in mind, one can readily explain the mare  
302 additive to form the FeO-MgO enriched agglutinitic glass of the Apollo 16 highlands.

303 Although we suggest that the source of the mafic glass component in highland soils is the  
304 maria in origin, an alternate source for the Apollo 16 soils might be the abundant “mafic impact  
305 melt breccias” thought to be derived from Imbrium [Korotev, 1997]. But, here we find it diffi-  
306 cult to address the scenario that these melt breccias were selectively and preferentially incorpo-  
307 rated into the Apollo 16 agglutinitic glass. Indeed, the Apollo 14 soil chemistry appears to reflect  
308 this possible Imbrium component, as seen from their higher K-phase (Fig. 1). However, the  
309 model we prefer is necessarily dependent on the small number of sites for which samples are  
310 available. It is obvious that we need samples from a highland site far-removed from any maria.

## 311 **8. Summary**

- 312 ◆ There is a general increase in agglutinitic glass content with decreasing grain size for the  
313 highland soils, exactly the same as with the mare soils.
- 314 ◆ The increase in  $I_S/\text{FeO}$  with decreasing grain size is greater than the abundance of agglutinitic  
315 glass: evidence of  $\text{np-Fe}^0$  on particle surfaces from vapor deposition (e.g., Hapke et al.,  
316 1975).
- 317 ◆ Agglutinitic glass is increased in plagioclase chemical components with decreasing grain  
318 size, typical of mare soils, however, not obvious for highland soils.

319 ◆ Apollo 16 agglutinitic glass chemistry contains more “mare-soil components” than the bulk-  
320 soil chemistry.

321 ◆ Mare agglutinitic glass appears to have been selectively added to the Apollo 16 soils, perhaps  
322 as impact ejecta and/or electrostatically transported fine-grained glass.

323

324

325 **Acknowledgements.** We would like to thank CAPTEM for the allocation of the pristine suite of  
326 highland soils. The Curatorial Staff at Johnson Space Center are also thanked for their efficient  
327 handling of the distribution of the numerous size fractions of the lunar soils, including the pro-  
328 duction of the polished grain mounts. We have benefited from fruitful discussions over the years  
329 with Paul Lucey, A. Basu, Sarah Noble, Jim Papike, Amy Riches, and Yang Liu. In addition, it  
330 has been the thorough reviews by Drs. Basu and Noble that have been extremely helpful in sub-  
331 stantially improving this paper. RELAB at Brown University is a multi-user facility supported  
332 under NAG 5-3871. The research presented in this paper was supported by NASA grants from  
333 the Cosmochemistry Program to each of the members of the Lunar Soil Characterization Consor-  
334 tium (LSCC), for which we are collectively appreciative.

335

336 **References**

- 337 Basu, A., and E. Molinaroli (2001) Sediments of the Moon and Earth as end-members for com-  
338 parative planetology. *Earth, Moon, & Planets* 85-86 25-43,
- 339 Basu, A., D.S. McKay, R.V. Morris, and S.J. Wentworth, (1996), Anatomy of individual aggluti-  
340 nates from a lunar highland soil, *Meteor. Planet. Sci.*, 31, 777-782.
- 341 Farrell, W. M., T. J. Stubbs, G. T. Delory, R. R. Vondrak, M. R. Collier, J. S. Halekas, and R. P.  
342 Lin (2008), Concerning the dissipation of electrically charged objects in the shadowed lunar  
343 polar regions, *Geophys. Res. Lett.*, 35, L19104, doi:10.1029/2008GL034785.
- 344 Hapke, B. (2001), Space weathering from Mercury to the asteroid belt. *Jour. Geophys. Res. –*  
345 *Planets* 106, 10,039-10,073.
- 346 Hapke, B., W.A. Cassidy, and E.N. Wells (1975), Effects of vapor-phase deposition processes on  
347 the optical, chemical, and magnetic properties of the lunar regolith, *Moon*, 13, 339-353
- 348 Hu, H.N., and L.A. Taylor (1977), Lack of chemical fractionation in major and minor elements  
349 during agglutinate formation, *Proc. Lunar Planet. Sci. Conf. 8th*, 3645-3656.
- 350 Keller, L.P., and D.S. McKay (1997), The nature and origin of rims on lunar soil grains, *Geo-*  
351 *chim. Cosmochim. Acta*, 61, 2331-2340.
- 352 Keller, L.P., S.J. Wentworth, D.S. McKay, L.A. Taylor, C.M. Pieters, and R.V. Morris R.V.  
353 (2000), Space weathering in the fine size fraction of lunar soils: Mare/highland differences,  
354 *Lunar Planet. Sci. Conf. [CD-Rom]*, XXXI, abstract 1655.
- 355 Korotev, R.L. (1997) Some things we can infer about the Moon from the composition of the  
356 Apollo 16 regolith. *Meteor. Planet. Sci.* 32, 447-478.
- 357 McGee, J.J. (1993), Lunar ferroan anorthosites' mineralogy, compositional variations, and petro-  
358 genesis. *Jour. Geophys. Res.* 98, 9089-9105,
- 359 Morris, R.V. (1976), Surface exposure indices of lunar soils: A comparative FMR study, *Proc.*  
360 *Lunar Planet Sci. Conf. 7th*, 315-335.
- 361 Morris, R.V. (1978), The surface exposure (mature) of lunar soils: Some concepts and Is/FeO  
362 compilation, *Proc. Lunar Planet. Sci. Conf. 9th*, 2287-2297.

363 Noble, S.K., C.M. Pieters, L.A. Taylor, R.V. Morris, C.C. Allen, D.S. McKay, and L.P. Keller  
364 (2001), The optical properties of the finest fraction of lunar soil: Implications for space wea-  
365 thering, *Meteor. Planet. Sci.*, 36, 31-42.

366 Noble, S.K., C.M. Pieters, and L.P. Keller (2007) An experimental approach to understanding the  
367 optical effects of space weathering. *Icarus* 192, 629-642.

368 Papike, J.J., S.B. Simon, C. White, and J.C. Laul (1982), The relationship of the lunar regolith  
369 <10  $\mu\text{m}$  fraction and agglutinates, Part I, A model for agglutinate formation and some indi-  
370 rect supportive evidence, *Proc. Lunar Planet. Sci.* 12, 409-420.

371 Pieters, C.M. (1983), Strength of mineral absorption features in the transmitted component of  
372 near-infrared reflected light: First results from RELAB, *J. Geophys. Res.*, 88, 9534-9544.

373 Pieters, C.M. (1993), Compositional diversity and stratigraphy of the lunar crust derived from  
374 reflectance spectroscopy, in *Remote Geochemical Analysis: Elemental and Mineralogical*  
375 *Composition.*, edited by [C. M. Pieters, and P.A.J. Englert ], 309-339, Cambridge Univ.  
376 Press, New York.

377 Pieters, C.M. and L.A. Taylor (2002), The perplexing role of  $\text{TiO}_2$  in the evolution of lunar soil.  
378 *Lunar & Planetary Sci. Conf. XXXIII*, LPI CD-ROM #1886.

379 Pieters, C.M., and L.A. Taylor (2003a), Systematic mixing and melting in lunar soil evolution.  
380 *Jour. Geophys. Lett.* 30, 20, 2048, doi:10.1029/2003GL018212.

381 Pieters, C.M., and L.A. Taylor (2003b), The Role of Agglutinates in Lunar Highland Soil Forma-  
382 tion , *Lunar & Planet. Sci. XXXIV*, LPI CD-ROM #1223.

383 Pieters, C.M., E.M. Fischer, O. Rode, and A. Basu (1993), Optical effects of space weathering:  
384 The role of the finest fraction, *J. Geophys. Res.* 98, 20,817-20,824.

385 Pieters, C.M., L.A. Taylor, S.K. Noble, L.P. Keller, B. Hapke, R.V. Morris, C.C. Allen, and S.  
386 Wentworth (2000), Space weathering on airless bodies: Resolving a mystery with lunar  
387 samples, *Meteor. Planet. Sci.*, 35, 1101-1107.

388 Pieters C.M., D.G. Stankevich, Y.G. Shkuratov, and L.A. Taylor (2001), Statistical analysis of  
389 lunar mare soil mineralogy, chemistry, and reflectance spectra, *Lunar Planet. Sci. Conf.*,  
390 [CD-Rom], XXXII, abstract 1783.

391 Pieters, C.M., D.G. Stankevich, Y.G. Shkuratov, and L.A. Taylor (2002), Statistical analysis of  
392 the links among lunar mare soil mineralogy, chemistry, and reflectance spectra, *Icarus* 155,  
393 285-298.

394 Taylor, L.A., and D.S. McKay (1992), Beneficiation of lunar rocks and regolith: Concepts and  
395 difficulties. In Engineering, Construction, Operations in Space III, Vol. I, Eds. Sadeh, Sture  
396 and Miller, ASCE, New York, 1058-1069.

397

398 Taylor, L.A., A. Patchen, D.-H. Taylor, J.G. Chambers, and D.S. McKay (1996), X-ray digital  
399 imaging and petrography of lunar mare soils: Data input for remote sensing calibrations, *Ica-*  
400 *rus*, 124, 500-512.

401 Taylor, L.A. C.M. Pieters, R.V. Morris, L.P. Keller, D.S. McKay, A. Patchen, and S.J. Went-  
402 worth (1999), Integration of the chemical and mineralogical characteristics of lunar soils  
403 with reflectance spectroscopy, *Proc., Lunar Planet. Sci. Conf.*, [CD-Rom], abstract, 1859.

404 Taylor, L.A., C.M. Pieters, L.P. Keller, R.V. Morris, D.S. McKay, A. Patchen, and S.J. Went-  
405 worth (2001a), The effects of space weathering on Apollo 17 mare soils: Petrographic and  
406 chemical characterization, *Meteor. Planet. Sci.*, 288-299.

407 Taylor, L.A., Pieters, C.M., Keller, L.P., Morris, R.V., and McKay, D.S. (2001b), Lunar mare  
408 soils: Space weathering and the major effects of surface-correlated nanophase Fe. *Jour.*  
409 *Geophys. Lett.* 106, 27,985-27,999.

410 Taylor, L.A., Cahill, J.T., Patchen, A., Pieters, C., Morris, R.V., Keller, L.P., & McKay, D.S.  
411 (2001c), Mineralogical and chemical characterization of lunar highland regolith: lessons  
412 learned from mare soils. *Lunar & Planetary Sci. Conf. XXXII*, LPI CD-OM # 2196.

413 Taylor, L.A., A. Patchen, J. Cahill1, C.M. Pieters, R.V. Morris, L.P. Keller, and D.S. Mckay  
414 (2002), Mineral and glass characterization of Apollo 14 soils. *Lunar & Planetary Sci. Conf.*  
415 XXXIII, LPI CD-ROM #1302.

416 Taylor, L.A., C.M. Pieters, A. Patchen, D.-H. Taylor, R.V. Morris, L.P. Keller, and D.S. McKay  
417 (2003), Mineralogical Characterization of Lunar Highland Soils, *Lunar & Planet. Sci.*  
418 XXXIV, LPI CD-ROM #1774.

419 Wentworth, S.J., L.P. Keller, D.S. McKay, and R.V. Morris (1999), Space weathering on the  
420 Moon: Patina on Apollo 17 samples 75075 and 76015, *Meteor. Planet. Sci.*, 34, 593-603.

421



## TABLES

422  
423  
424  
  
425  
426  
427  
428  
  
429  
430  
431  
432  
  
433  
434  
435  
436  
437  
438  
  
439  
440  
441  
442  
443

Table 1. Lunar highland soils studies by the Lunar Soil Characterization Consortium (LSCC).

Table 2. Modal abundance of minerals and glasses in finest size fractions of selected Apollo Highland Soils. Maturity as  $I_s/FeO$  of the  $<250 \mu m$  fraction [Morris, 1978] is given directly after the soil number, a value commonly used as the reference maturity for an entire soil.

Table 3. Modal percentages of four sub-sets of pyroxenes in the finest size fractions of Apollo Highland soils. Maturity as  $I_s/FeO$  of the  $<250 \mu m$  fraction [Morris, 1978] is given directly after the soil number, a value commonly used as the reference maturity for an entire soil.

Table 4. Bulk chemistry and  $I_s/FeO$  values of the finest size fractions of Apollo Highland Soils. The chemistry was determined by EMP analyses of fused beads of the soil. Values of  $I_s/FeO$  are from FMR analyses. Maturity as  $I_s/FeO$  of the  $<250 \mu m$  fraction [Morris, 1978] is given directly after the soil number, a value commonly used as the reference maturity for an entire soil.

Table 5. Average compositions of minerals and glasses in the finest size fractions of Apollo Highland soils. Maturity as  $I_s/FeO$  of the  $<250 \mu m$  fraction [Morris, 1978] is given directly after the soil number, a value commonly used as the reference maturity for an entire soil. Values in brackets are the 2 sigma error.

444  
445

## FIGURES

446  
447  
  
448  
449  
  
450  
451  
452  
  
453  
454  
455

Figure 1. Modal analyses of phases in the fine fractions of highland soils. These data are modified after those in a LPSC abstract [Taylor et al., 2003].

Figure 2. Comparisons of oxide components of the bulk chemistry of the fine fractions of highland soils, in addition to their  $I_s/FeO$  values

Figure 3. Comparison of chemistry of the agglutinitic glass with the bulk chemistry of the three soil size fractions for Apollo 16 highland soils. Modified from LPSC abstract [Taylor et al., 2003].

Figure 4. Chemistry of soil components relative to the chemistry of the bulk soil ( $<45 \mu m$ ) for representative highland soils. The first three bars (blue shades) are the composition of three soil size separates (see legend). These are followed by the average composition

456 of agglutinitic glass (red shades) present in the indicated size separate. The number in  
457 brackets is the  $I_s/FeO$  value for the bulk soil from Morris [1978]. Some of these data  
458 have been reported in Pieters and Taylor [2003a].

459 Figure 5. Bi-directional reflectance spectra of LSCC highland soils. Data for 64801 are from  
460 Pieters and Taylor [2003a].

461

462 TABLE 1. Lunar Highland Soils Studied by the Lunar Soil Characterization Consortium  
 463 (LSCC).

464

<b>SAMPLES</b>		<b>Is / FeO*</b>	<b>MATURITY**</b>
<b>Apollo 16</b>	<b>61221</b>	<b>9</b>	<b>I</b>
	<b>67461</b>	<b>25</b>	<b>I</b>
	<b>67481</b>	<b>31</b>	<b>S</b>
	<b>61141</b>	<b>56</b>	<b>S</b>
	<b>64801</b>	<b>71</b>	<b>M</b>
	<b>62231</b>	<b>91</b>	<b>M</b>
<b>Apollo 14</b>	<b>14141</b>	<b>6</b>	<b>I</b>
	<b>14163</b>	<b>57</b>	<b>M</b>
	<b>14260</b>	<b>72</b>	<b>M</b>
	<b>14259</b>	<b>85</b>	<b>M</b>

465

466 \* Values from compilation of Morris [1978] for the <250 μm portion of each soil;

467 \*\* Maturity based on I<sub>s</sub>/FeO [10]; I = Immature = <30 ;

468 S = Submature = 30-60 ; M = Mature = >60.

469

470

471

472 Table 2. Modal abundance of minerals and glasses in finest size fractions of selected Apollo Highland Soils. Maturity as  $I_S/FeO$  of the  
 473 <250  $\mu m$  fraction [Morris, 1978] is given directly after the soil number, a value commonly used as the reference maturity for an entire  
 474 soil.  
 475

	<b>14141<sup>-5.7</sup></b>			<b>14163<sup>-57</sup></b>			<b>14260<sup>-72</sup></b>			<b>14259<sup>-85</sup></b>		
	<b>20-45<math>\mu m</math></b>	<b>10-20<math>\mu m</math></b>	<b>&lt;10<math>\mu m</math></b>	<b>20-45<math>\mu m</math></b>	<b>10-20<math>\mu m</math></b>	<b>&lt;10<math>\mu m</math></b>	<b>20-45<math>\mu m</math></b>	<b>10-20<math>\mu m</math></b>	<b>&lt;10<math>\mu m</math></b>	<b>20-45<math>\mu m</math></b>	<b>10-20<math>\mu m</math></b>	<b>&lt;10<math>\mu m</math></b>
<b>Agglut. Glass</b>	41.0	48.6	45.9	56.4	58.5	66.3	64.0	65.2	66.5	60.5	68.7	71.6
<b>Pyroxene</b>	19.8	10.9	10.3	16.2	13.8	3.8	13.7	12.1	7.7	18.2	9.1	5.9
<b>Plag</b>	26.6	28.0	27.6	18.9	18.3	21.8	15.6	16.1	16.3	14.1	15.4	14.6
<b>Olivine</b>	4.0	1.6	1.5	2.4	2.1	0.4	2.1	1.5	1.4	2.3	1.4	0.7
<b>Ilmenite</b>	1.9	1.1	1.7	0.8	0.9	1.1	0.9	1.0	1.3	1.3	1.2	1.5
<b>K-Phases</b>	4.5	7.4	10.8	3.8	4.1	3.4	2.5	2.6	3.7	2.5	2.7	3.4
<b>Others</b>	2.2	2.4	2.2	1.5	2.3	3.2	1.2	1.5	3.1	1.1	1.5	2.3
<b>Total</b>	<b>100.0</b>	<b>100.0</b>	<b>100.0</b>	<b>100.0</b>	<b>100.0</b>	<b>100.0</b>	<b>100.0</b>	<b>100.0</b>	<b>100.0</b>	<b>100.0</b>	<b>100.0</b>	<b>100.0</b>

476  
477

	<b>61221<sup>-9.2</sup></b>			<b>67461<sup>-25</sup></b>			<b>67481<sup>-31</sup></b>			<b>61141<sup>-56</sup></b>		
	<b>20-45<math>\mu m</math></b>	<b>10-20<math>\mu m</math></b>	<b>&lt;10<math>\mu m</math></b>	<b>20-45<math>\mu m</math></b>	<b>10-20<math>\mu m</math></b>	<b>&lt;10<math>\mu m</math></b>	<b>20-45<math>\mu m</math></b>	<b>10-20<math>\mu m</math></b>	<b>&lt;10<math>\mu m</math></b>	<b>20-45<math>\mu m</math></b>	<b>10-20<math>\mu m</math></b>	<b>&lt;10<math>\mu m</math></b>
<b>Agglut. Glass</b>	28.9	32.6	41.6	25.4	32.4	35.8	27.6	28.6	35.2	50.1	53.9	61.6
<b>Pyroxene</b>	7.4	5.3	1.5	7.3	4.1	2.8	6.6	5.6	3.6	4.4	3.3	1.7
<b>Plag</b>	58.7	59.4	54.4	64.3	61.0	60.0	61.2	62.0	58.8	42.5	40.3	35.3
<b>Olivine</b>	3.9	2.0	0.9	2.5	1.5	0.7	4.0	2.9	1.5	2.1	1.6	0.5
<b>Ilmenite</b>	0.6	0.3	0.9	0.3	0.3	0.2	0.1	0.2	0.2	0.3	0.3	0.3
<b>K-Phases</b>	0.2	0.2	0.3	0.1	0.2	0.1	0.3	0.4	0.3	0.3	0.4	0.3
<b>Others</b>	0.3	0.2	0.4	0.1	0.5	0.4	0.2	0.3	0.4	0.3	0.2	0.3
<b>Total</b>	<b>100.0</b>	<b>100.0</b>	<b>100.0</b>	<b>100.0</b>	<b>100.0</b>	<b>100.0</b>	<b>100.0</b>	<b>100.0</b>	<b>100.0</b>	<b>100.0</b>	<b>100.0</b>	<b>100.0</b>

478

	<b>64801<sup>-82</sup></b>			<b>62231<sup>-91</sup></b>		
	<b>20-45<math>\mu m</math></b>	<b>10-20<math>\mu m</math></b>	<b>&lt;10<math>\mu m</math></b>	<b>20-45<math>\mu m</math></b>	<b>10-20<math>\mu m</math></b>	<b>&lt;10<math>\mu m</math></b>
<b>Agglut. Glass</b>	53.6	61.0	63.6	50.6	55.0	69.5
<b>Pyroxene</b>	4.5	2.8	2.7	5.1	4.40	0.9
<b>Plag</b>	39.3	34.5	32.3	40.5	37.8	28.3
<b>Olivine</b>	1.8	1.0	0.6	2.9	1.7	0.3
<b>Ilmenite</b>	0.3	0.2	0.2	0.3	0.5	0.4
<b>K-Phases</b>	0.3	0.3	0.4	0.3	0.4	0.3
<b>Others</b>	0.2	0.2	0.2	0.3	0.2	0.3
<b>Total</b>	<b>100.0</b>	<b>100.0</b>	<b>100.0</b>	<b>100.0</b>	<b>100.0</b>	<b>100.0</b>

479

480 Table 3. Modal percentages of four sub-sets of pyroxenes in the finest size fractions of Apollo Highland soils. Maturity as  $I_s/FeO$  of the  
 481 <250  $\mu m$  fraction [Morris, 1978] is given directly after the soil number, a value commonly used as the reference maturity for an entire  
 482 soil.

483

	<b>14141-5.7</b>			<b>14163-57</b>			<b>14260-72</b>			<b>14259-85</b>		
	<b>20-45<math>\mu m</math></b>	<b>10-20<math>\mu m</math></b>	<b>&lt;10<math>\mu m</math></b>	<b>20-45<math>\mu m</math></b>	<b>10-20<math>\mu m</math></b>	<b>&lt;10<math>\mu m</math></b>	<b>20-45<math>\mu m</math></b>	<b>10-0<math>\mu m</math></b>	<b>&lt;10<math>\mu m</math></b>	<b>20-45<math>\mu m</math></b>	<b>10-20<math>\mu m</math></b>	<b>&lt;10<math>\mu m</math></b>
<b>Orthopyroxene</b>	7.57	4.07	3.37	6.50	5.68	1.51	4.68	5.14	2.58	7.40	3.72	1.92
<b>Pigeonite</b>	8.08	4.58	4.29	5.66	4.94	1.38	4.99	4.23	3.15	6.14	3.18	1.96
<b>Mg-Clinopyroxene</b>	3.08	1.85	2.19	3.10	2.41	0.91	3.07	2.00	1.51	3.04	1.66	1.77
<b>Fe-Pyroxene</b>	1.08	0.38	0.44	0.92	0.78	0.14	0.94	0.64	0.48	1.57	0.50	0.29
<b>Total Pyroxene</b>	19.81	10.88	10.29	16.18	13.81	3.94	13.68	12.01	7.72	18.15	9.06	5.94

484

	<b>61221-9.2</b>			<b>67461-25</b>			<b>67481-31</b>			<b>61141-56</b>		
	<b>20-45<math>\mu m</math></b>	<b>10-20<math>\mu m</math></b>	<b>&lt;10<math>\mu m</math></b>	<b>20-45<math>\mu m</math></b>	<b>10-20<math>\mu m</math></b>	<b>&lt;10<math>\mu m</math></b>	<b>20-45<math>\mu m</math></b>	<b>10-0<math>\mu m</math></b>	<b>&lt;10<math>\mu m</math></b>	<b>20-45<math>\mu m</math></b>	<b>10-20<math>\mu m</math></b>	<b>&lt;10<math>\mu m</math></b>
<b>Orthopyroxene</b>	2.96	1.82	0.56	2.96	1.47	1.09	2.95	2.55	1.38	1.68	1.69	0.22
<b>Pigeonite</b>	2.24	1.43	0.55	1.61	1.07	0.64	1.54	1.27	1.05	1.38	2.15	0.23
<b>Mg-Clinopyroxene</b>	1.98	1.95	0.37	2.53	1.52	1.06	1.94	1.73	1.41	1.11	1.45	0.19
<b>Fe-Pyroxene</b>	0.19	0.14	0.02	0.18	0.05	0.04	0.17	0.13	0.05	0.18	0.04	0.06
<b>Total Pyroxene</b>	7.37	5.34	1.50	7.28	4.11	2.83	6.60	5.68	3.89	4.35	5.33	0.70

486

	<b>64801-82</b>			<b>62231-91</b>		
	<b>20-45<math>\mu m</math></b>	<b>10-20<math>\mu m</math></b>	<b>&lt;10<math>\mu m</math></b>	<b>20-45<math>\mu m</math></b>	<b>10-20<math>\mu m</math></b>	<b>&lt;10<math>\mu m</math></b>
<b>Orthopyroxene</b>	2.03	1.24	1.18	2.08	1.99	0.28
<b>Pigeonite</b>	1.15	0.96	0.84	1.33	1.55	0.27
<b>Mg-Clinopyroxene</b>	1.33	0.60	0.64	1.52	1.74	0.30
<b>Fe-Pyroxene</b>	0.01	0.01	0.00	0.19	0.12	0.03
<b>Total Pyroxene</b>	4.52	2.81	2.66	5.12	5.40	0.88

487

488

489  
490  
491  
492

Table 4. Bulk chemistry and  $I_s/FeO$  values of the finest size fractions of Apollo Highland Soils. The chemistry was determined by EMP analyses of fused beads of the soil. Values of  $I_s/FeO$  are from FMR analyses. Maturity as  $I_s/FeO$  of the  $<250 \mu m$  fraction [Morris, 1978] is given directly after the soil number, a value commonly used as the reference maturity for an entire soil.

Sample	14141-5.7				14163-57				14260-72			
	<45 $\mu m$	20-45 $\mu m$	10-20 $\mu m$	<10 $\mu m$	<45 $\mu m$	20-45 $\mu m$	10-20 $\mu m$	<10 $\mu m$	<45 $\mu m$	20-45 $\mu m$	10-20 $\mu m$	<10 $\mu m$
SiO <sub>2</sub>	47.9	47.2	48.4	49.2	47.4	47.1	47.4	47.2	47.6	47.4	47.5	47.8
TiO <sub>2</sub>	1.65	1.96	1.71	1.51	1.90	2.00	1.88	2.07	1.85	1.86	1.98	1.94
Al <sub>2</sub> O <sub>3</sub>	17.0	15.0	17.2	19.2	17.1	15.4	17.0	18.9	17.3	16.3	17.3	19.1
Cr <sub>2</sub> O <sub>3</sub>	0.22	0.26	0.23	0.21	0.20	0.23	0.22	0.21	0.21	0.22	0.23	0.20
MgO	9.28	11.0	9.08	6.99	9.49	11.0	9.57	8.14	9.46	10.4	9.53	8.21
CaO	10.7	10.1	10.7	11.3	10.9	10.2	10.8	11.6	11.0	10.7	11.0	11.8
MnO	0.14	0.15	0.13	0.10	0.15	0.15	0.13	0.12	0.15	0.14	0.13	0.12
FeO	9.81	11.6	9.46	7.66	9.94	11.5	10.1	8.83	9.65	10.7	9.84	8.10
Na <sub>2</sub> O	0.76	0.59	0.71	0.91	0.65	0.57	0.67	0.70	0.61	0.60	0.60	0.57
K <sub>2</sub> O	0.70	0.47	0.66	0.96	0.51	0.41	0.51	0.55	0.49	0.44	0.46	0.47
P <sub>2</sub> O <sub>5</sub>	0.50	0.26	0.32	0.40	0.35	0.21	0.27	0.33	0.32	0.22	0.21	0.17
SO <sub>3</sub>	0.10	0.07	0.07	0.10	0.10	0.08	0.10	0.11	0.12	0.10	0.10	0.09
Total	<b>98.82</b>	<b>98.78</b>	<b>98.68</b>	<b>98.61</b>	<b>98.69</b>	<b>99.02</b>	<b>98.72</b>	<b>98.85</b>	<b>98.81</b>	<b>99.13</b>	<b>98.97</b>	<b>98.76</b>
$I_s/FeO$	<b>9.7</b>	<b>5.8</b>	<b>11.6</b>	<b>14.5</b>	<b>66.5</b>	<b>43.2</b>	<b>64.8</b>	<b>87.0</b>	<b>93.3</b>	<b>80.2</b>	<b>98.9</b>	<b>144.9</b>

493  
494

Sample	14259-85				61221-9.2				67461-25			
	<45 $\mu m$	20-45 $\mu m$	10-20 $\mu m$	<10 $\mu m$	<45 $\mu m$	20-45 $\mu m$	10-20 $\mu m$	<10 $\mu m$	<45 $\mu m$	20-45 $\mu m$	10-20 $\mu m$	<10 $\mu m$
SiO <sub>2</sub>	47.7	47.1	47.5	47.9	44.7	44.5	44.5	44.5	44.6	44.4	44.1	44.5
TiO <sub>2</sub>	1.80	1.99	1.96	2.02	0.52	0.56	0.54	0.50	0.35	0.44	0.39	0.34
Al <sub>2</sub> O <sub>3</sub>	17.4	15.8	17.4	19.3	27.3	27.2	27.5	28.5	28.4	27.3	27.8	29.4
Cr <sub>2</sub> O <sub>3</sub>	0.20	0.24	0.23	0.20	0.09	0.09	0.09	0.08	0.08	0.09	0.08	0.08
MgO	9.47	10.7	9.44	8.09	5.29	5.45	5.16	4.35	4.46	5.11	4.80	3.83
CaO	11.1	10.5	11.0	11.9	15.9	15.9	16.0	16.5	16.5	16.1	16.5	17.1
MnO	0.13	0.15	0.13	0.12	0.08	0.06	0.05	0.06	0.06	0.07	0.08	0.06
FeO	9.54	11.0	9.71	7.82	4.47	4.62	4.40	3.64	4.24	4.93	4.64	3.35
Na <sub>2</sub> O	0.62	0.60	0.63	0.63	0.48	0.46	0.45	0.53	0.40	0.41	0.39	0.43
K <sub>2</sub> O	0.47	0.43	0.47	0.50	0.09	0.07	0.09	0.13	0.06	0.05	0.05	0.07
P <sub>2</sub> O <sub>5</sub>	0.30	0.26	0.23	0.23	0.06	0.05	0.05	0.06	0.04	0.03	0.04	0.03
SO <sub>3</sub>	0.11	0.09	0.12	0.10	0.07	0.04	0.06	0.10	0.06	0.07	0.04	0.07
Total	<b>98.80</b>	<b>99.02</b>	<b>98.87</b>	<b>98.84</b>	<b>99.13</b>	<b>99.07</b>	<b>98.93</b>	<b>99.00</b>	<b>99.26</b>	<b>99.00</b>	<b>98.90</b>	<b>99.31</b>
$I_s/FeO$	<b>108.6</b>	<b>77.2</b>	<b>101.8</b>	<b>174.8</b>	<b>13.6</b>	<b>8.4</b>	<b>13.89</b>	<b>19.8</b>	<b>29.8</b>	<b>22.3</b>	<b>23.9</b>	<b>35.2</b>

495  
496  
497  
498  
499

500

501  
502  
503

Table 4 continued

Sample	67481-31				61141-56				64801-82			
	<45µm	20-45µm	10-20µm	<10µm	<45µm	20-45µm	10-20µm	<10µm	<45µm	20-45µm	10-20µm	<10µm
SiO <sub>2</sub>	44.6	44.7	44.4	44.5	45.0	44.5	44.6	44.9	45.0	44.6	44.5	44.8
TiO <sub>2</sub>	0.44	0.49	0.40	0.42	0.59	0.58	0.64	0.59	0.65	0.63	0.68	0.61
Al <sub>2</sub> O <sub>3</sub>	28.1	26.7	28.4	29.1	26.3	26.1	25.6	27.4	26.9	26.5	26.3	27.7
Cr <sub>2</sub> O <sub>3</sub>	0.10	0.09	0.09	0.08	0.12	0.11	0.13	0.11	0.10	0.10	0.12	0.12
MgO	4.91	5.98	4.54	4.09	6.39	6.56	6.84	5.53	5.83	6.09	6.18	5.22
CaO	16.2	15.6	16.4	16.7	15.3	15.2	15.2	16.0	15.6	15.6	15.6	16.1
MnO	0.06	0.08	0.05	0.07	0.07	0.08	0.08	0.07	0.06	0.08	0.08	0.07
FeO	4.38	5.19	4.04	3.61	4.80	5.15	5.14	3.66	4.68	4.82	4.78	3.84
Na <sub>2</sub> O	0.43	0.45	0.45	0.46	0.43	0.46	0.41	0.48	0.43	0.44	0.41	0.42
K <sub>2</sub> O	0.06	0.06	0.07	0.08	0.11	0.10	0.10	0.14	0.12	0.12	0.11	0.14
P <sub>2</sub> O <sub>5</sub>	0.04	0.05	0.04	0.04	0.06	0.06	0.05	0.06	0.07	0.06	0.06	0.04
SO <sub>3</sub>	0.04	0.04	0.06	0.07	0.09	0.05	0.08	0.11	0.09	0.10	0.07	0.11
<b>Total</b>	<b>99.39</b>	<b>99.50</b>	<b>99.08</b>	<b>99.22</b>	<b>99.34</b>	<b>99.00</b>	<b>98.91</b>	<b>99.11</b>	<b>99.50</b>	<b>99.20</b>	<b>98.99</b>	<b>99.21</b>
<b>I<sub>s</sub>/FeO</b>	<b>33.5</b>	<b>20.7</b>	<b>33.0</b>	<b>38.5</b>	<b>94.5</b>	<b>75.5</b>	<b>81.6</b>	<b>119.3</b>	<b>92.2</b>	<b>83.4</b>	<b>84.9</b>	<b>115.2</b>

504

Sample	62231-91			
	<45µm	20-45µm	10-20µm	<10µm
SiO <sub>2</sub>	45.0	44.5	44.7	45.0
TiO <sub>2</sub>	0.60	0.58	0.61	0.58
Al <sub>2</sub> O <sub>3</sub>	26.3	25.7	26.3	27.4
Cr <sub>2</sub> O <sub>3</sub>	0.11	0.11	0.13	0.13
MgO	6.20	6.59	6.38	5.49
CaO	15.4	15.3	15.5	16.1
MnO	0.09	0.09	0.07	0.07
FeO	4.87	5.31	4.86	3.63
Na <sub>2</sub> O	0.43	0.42	0.41	0.46
K <sub>2</sub> O	0.12	0.09	0.10	0.14
P <sub>2</sub> O <sub>5</sub>	0.07	0.07	0.05	0.04
SO <sub>3</sub>	0.09	0.08	0.08	0.13
<b>Total</b>	<b>99.32</b>	<b>98.87</b>	<b>99.22</b>	<b>99.22</b>
<b>I<sub>s</sub>/FeO</b>	<b>116.7</b>	<b>80.7</b>	<b>109.9</b>	<b>169.0</b>

505  
506

507 Table 5. Average compositions of minerals and glasses in the finest size fractions of Apollo Highland soils.  
 508 Maturity as  $I_5/FeO$  of the <250  $\mu m$  fraction [Morris, 1978] is given directly after the soil number, a value commonly used as the reference  
 509 maturity for an entire soil. Values in brackets are the 2 sigma error.

510

<b>14141 -5.7 (20-45<math>\mu m</math>)</b>									
	<b>Plag</b>	<b>Ilm</b>	<b>Olivine</b>	<b>K-glass</b>	<b>Agglut. Gls.</b>	<b>Opx</b>	<b>Pig</b>	<b>Mg-Cpx</b>	<b>Fe-Cpx</b>
<b>SiO<sub>2</sub></b>	45.7	<0.04	36.2	70.1	47.0 (37)	52.8	51.6	49.9	46.9
<b>TiO<sub>2</sub></b>	<0.04	52.4	0.07	0.27	1.82 (208)	0.68	0.74	1.30	1.06
<b>Al<sub>2</sub>O<sub>3</sub></b>	33.5	0.10	0.06	13.7	17.9 (75)	1.03	1.51	1.74	1.32
<b>Cr<sub>2</sub>O<sub>3</sub></b>	<0.04	0.61	0.08	<0.04	0.18 (11)	0.36	0.47	0.46	0.21
<b>MgO</b>	0.09	3.42	31.8	0.31	7.98 (441)	24.6	20.5	13.8	6.72
<b>CaO</b>	17.6	0.17	0.15	1.16	11.4 (34)	1.84	4.59	15.1	10.3
<b>FeO</b>	0.06	40.8	30.1	1.21	9.76 (608)	17.3	19.0	16.0	30.9
<b>Na<sub>2</sub>O</b>	1.22	<0.04	<0.04	0.86	0.74 (51)	<0.04	<0.04	0.07	<0.04
<b>K<sub>2</sub>O</b>	0.16	<0.04	<0.04	8.81	0.46 (54)	<0.04	<0.04	<0.04	<0.04
<b>Total</b>	<b>98.33</b>	<b>97.50</b>	<b>98.46</b>	<b>96.42</b>	<b>97.24</b>	<b>98.61</b>	<b>98.41</b>	<b>98.37</b>	<b>97.41</b>

511  
512

<b>14141 -5.7 (10-20 <math>\mu m</math>)</b>									
	<b>Plag</b>	<b>Ilm</b>	<b>Olivine</b>	<b>K-glass</b>	<b>Agglut. Gls.</b>	<b>Opx</b>	<b>Pig</b>	<b>Mg-Cpx</b>	<b>Fe-Cpx</b>
<b>SiO<sub>2</sub></b>	45.2	<0.04	36.6	72.0	46.8 (41)	52.7	51.7	50.0	46.7
<b>TiO<sub>2</sub></b>	0.06	52.3	0.11	0.39	1.69 (180)	0.76	0.78	1.51	1.23
<b>Al<sub>2</sub>O<sub>3</sub></b>	34.0	0.14	0.14	12.1	19.3 (64)	1.02	1.37	1.98	1.39
<b>Cr<sub>2</sub>O<sub>3</sub></b>	<0.04	0.56	0.08	<0.04	0.20 (12)	0.34	0.45	0.56	0.18
<b>MgO</b>	0.13	3.33	32.8	0.12	7.91 (369)	24.2	20.6	14.6	5.73
<b>CaO</b>	18.0	0.20	0.15	1.96	11.9 (32)	1.99	4.33	16.2	10.6
<b>FeO</b>	0.17	40.6	28.9	3.31	8.81 (417)	17.4	19.2	13.0	31.8
<b>Na<sub>2</sub>O</b>	1.07	<0.04	<0.04	1.49	0.74 (59)	<0.04	<0.04	0.10	<0.04
<b>K<sub>2</sub>O</b>	0.15	0.05	<0.04	5.45	0.39 (41)	<0.04	<0.04	<0.04	<0.04
<b>Total</b>	<b>98.78</b>	<b>97.18</b>	<b>98.78</b>	<b>96.82</b>	<b>97.80</b>	<b>98.41</b>	<b>98.43</b>	<b>97.95</b>	<b>97.63</b>

513  
514



515  
516  
517

**Table 5. Continued**

<b>14163 -57 (20-45µm)</b>									
	<b>Plag</b>	<b>Ilm</b>	<b>Olivine</b>	<b>K-glass</b>	<b>Agglut. Gls.</b>	<b>Opx</b>	<b>Pig</b>	<b>Mg-Cpx</b>	<b>Fe-Cpx</b>
<b>SiO<sub>2</sub></b>	46.2	<0.04	36.7	67.6	46.8 (30)	52.9	51.5	50.6	46.8
<b>TiO<sub>2</sub></b>	0.04	51.6	0.08	0.43	1.71 (138)	0.75	0.67	1.27	0.94
<b>Al<sub>2</sub>O<sub>3</sub></b>	32.9	0.16	0.04	14.8	17.2 (61)	1.30	1.46	1.70	1.01
<b>Cr<sub>2</sub>O<sub>3</sub></b>	<0.04	0.65	0.05	<0.04	0.17 (13)	0.32	0.39	0.39	0.12
<b>MgO</b>	0.04	2.17	34.3	0.54	8.64 (394)	24.2	18.1	13.9	4.97
<b>CaO</b>	17.6	0.25	0.16	2.25	11.4 (28)	2.00	5.17	16.6	11.0
<b>FeO</b>	0.06	42.3	26.8	1.90	10.2 (49)	16.8	21.0	13.8	32.7
<b>Na<sub>2</sub>O</b>	1.38	<0.04	<0.04	1.21	0.58 (39)	<0.04	0.04	0.13	0.05
<b>K<sub>2</sub>O</b>	0.18	0.04	<0.04	8.40	0.43 (44)	<0.04	<0.04	<0.04	<0.04
<b>Total</b>	<b>98.4</b>	<b>97.17</b>	<b>98.13</b>	<b>97.13</b>	<b>97.03</b>	<b>98.27</b>	<b>98.33</b>	<b>98.39</b>	<b>97.59</b>

518  
519  
520

<b>14163 -57 (10-20µm)</b>									
	<b>Plag</b>	<b>Ilm</b>	<b>Olivine</b>	<b>Vol Gls.</b>	<b>Agglut. Gls.</b>	<b>Opx</b>	<b>Pig</b>	<b>Mg-Cpx</b>	<b>Fe-Cpx</b>
<b>SiO<sub>2</sub></b>	45.8	0.12	36.8	67.9	46.4 (28)	52.9	51.4	50.4	47.6
<b>TiO<sub>2</sub></b>	<0.04	52.0	0.08	0.30	1.66 (123)	0.75	0.68	1.38	1.04
<b>Al<sub>2</sub>O<sub>3</sub></b>	33.6	0.19	0.09	15.2	18.1 (63)	1.10	1.18	1.90	1.24
<b>Cr<sub>2</sub>O<sub>3</sub></b>	<0.04	0.45	0.11	<0.04	0.19 (37)	0.31	0.38	0.48	0.18
<b>MgO</b>	0.08	3.95	33.3	0.14	8.64 (353)	24.8	19.4	14.7	7.52
<b>CaO</b>	17.6	0.26	0.24	1.73	11.6 (28)	1.88	4.68	17.2	10.8
<b>FeO</b>	0.22	39.5	27.9	1.83	9.65 (438)	16.4	20.3	12.1	29.0
<b>Na<sub>2</sub>O</b>	1.33	<0.04	<0.04	1.23	0.59 (40)	<0.04	<0.04	0.13	0.06
<b>K<sub>2</sub>O</b>	0.14	<0.04	<0.04	8.64	0.36 (39)	<0.04	<0.04	<0.04	<0.04
<b>Total</b>	<b>98.77</b>	<b>96.47</b>	<b>98.52</b>	<b>96.97</b>	<b>97.19</b>	<b>98.14</b>	<b>98.02</b>	<b>98.29</b>	<b>97.44</b>

521  
522

523  
524  
525  
526  
527

Table 5. Cont.

<b>14260 -72 (20-45µm)</b>									
	<b>Plag</b>	<b>Ilm</b>	<b>Olivine</b>	<b>Vol Gls.</b>	<b>Agglut. Gls.</b>	<b>Opx</b>	<b>Pig</b>	<b>Mg-Cpx</b>	<b>Fe-Cpx</b>
<b>SiO<sub>2</sub></b>	45.6	0.07	36.7	68.6	46.3 (37)	52.8	50.9	50.1	47.1
<b>TiO<sub>2</sub></b>	0.05	52.4	0.09	0.38	1.54 (113)	0.79	0.88	1.50	1.01
<b>Al<sub>2</sub>O<sub>3</sub></b>	33.7	0.06	0.05	15.8	18.6 (66)	1.06	1.63	2.10	1.15
<b>Cr<sub>2</sub>O<sub>3</sub></b>	<0.04	0.50	0.12	<0.04	0.21 (15)	0.35	0.47	0.58	0.24
<b>MgO</b>	0.09	3.54	32.8	0.10	8.42 (418)	24.5	18.3	14.7	6.91
<b>CaO</b>	17.6	0.19	0.17	2.07	11.6 (31)	1.86	5.28	16.6	12.3
<b>FeO</b>	0.18	40.5	29.1	0.27	9.64 (487)	17.3	21.1	12.6	28.6
<b>Na<sub>2</sub>O</b>	1.22	<0.04	<0.04	1.09	0.60 (45)	<0.04	<0.04	0.12	0.0
<b>K<sub>2</sub>O</b>	0.14	<0.04	<0.04	8.96	0.41 (45)	<0.04	<0.04	<0.04	<0.04
<b>Total</b>	<b>98.58</b>	<b>97.26</b>	<b>99.03</b>	<b>97.27</b>	<b>97.26</b>	<b>98.66</b>	<b>98.56</b>	<b>98.30</b>	<b>97.31</b>

528  
529  
530

<b>14260 -72 (10-20µm)</b>									
	<b>Plag</b>	<b>Ilm</b>	<b>Olivine</b>	<b>Vol Gls.</b>	<b>Agglut. Gls.</b>	<b>Opx</b>	<b>Pig</b>	<b>Mg-Cpx</b>	<b>Fe-Cpx</b>
<b>SiO<sub>2</sub></b>	45.8	0.10	36.9	66.3	45.5 (44)	53.0	51.1	50.8	47.8
<b>TiO<sub>2</sub></b>	0.05	51.3	0.10	0.32	1.62 (125)	0.80	0.82	1.30	1.12
<b>Al<sub>2</sub>O<sub>3</sub></b>	33.8	0.18	0.08	15.6	19.9 (71)	1.04	1.17	1.89	1.37
<b>Cr<sub>2</sub>O<sub>3</sub></b>	<0.04	0.53	0.09	<0.04	0.22 (11)	0.32	0.33	0.50	0.18
<b>MgO</b>	0.08	3.25	32.9	0.61	8.39 (401)	24.1	18.6	15.0	7.01
<b>CaO</b>	17.6	0.24	0.19	2.31	12.4 (34)	1.92	4.94	16.4	12.7
<b>FeO</b>	0.28	40.8	29.2	2.05	8.85 (434)	17.9	21.4	12.9	28.1
<b>Na<sub>2</sub>O</b>	1.28	<0.04	<0.04	0.79	0.53 (42)	<0.04	<0.04	0.08	<0.04
<b>K<sub>2</sub>O</b>	0.15	0.06	<0.04	8.42	0.40 (48)	<0.04	<0.04	<0.04	<0.04
<b>Total</b>	<b>99.04</b>	<b>97.46</b>	<b>99.46</b>	<b>96.40</b>	<b>97.90</b>	<b>99.08</b>	<b>98.36</b>	<b>98.87</b>	<b>98.28</b>

531  
532  
533

534  
535  
536  
537  
538

**Table 5. Cont.**

<b>14259 -85 (20-45µm)</b>									
	<b>Plag</b>	<b>Ilm</b>	<b>Olivine</b>	<b>Vol Gls.</b>	<b>Agglut. Gls.</b>	<b>Opx</b>	<b>Pig</b>	<b>Mg-Cpx</b>	<b>Fe-Cpx</b>
<b>SiO<sub>2</sub></b>	46.3	<0.04	36.9	68.7	46.5 (33)	53.0	51.4	50.3	46.9
<b>TiO<sub>2</sub></b>	0.05	52.8	0.10	0.69	1.50 (118)	0.75	0.75	1.42	1.01
<b>Al<sub>2</sub>O<sub>3</sub></b>	33.5	0.09	0.06	14.8	19.2 (63)	0.98	1.22	2.00	1.09
<b>Cr<sub>2</sub>O<sub>3</sub></b>	<0.04	0.52	0.11	<0.04	0.19 (11)	0.35	0.44	0.53	0.19
<b>MgO</b>	0.10	3.23	33.1	0.21	8.38 (378)	24.5	19.0	14.6	5.03
<b>CaO</b>	17.3	0.11	0.18	1.82	12.0 (29)	1.83	5.10	16.2	11.2
<b>FeO</b>	0.05	41.1	28.8	1.30	9.17 (459)	17.5	20.7	13.3	32.5
<b>Na<sub>2</sub>O</b>	1.41	<0.04	<0.04	1.02	0.61 (66)	<0.04	<0.04	0.11	<0.04
<b>K<sub>2</sub>O</b>	0.20	<0.04	<0.04	8.57	0.37 (43)	<0.04	<0.04	<0.04	<0.04
<b>Total</b>	<b>98.91</b>	<b>97.85</b>	<b>99.25</b>	<b>97.11</b>	<b>97.80</b>	<b>98.91</b>	<b>98.61</b>	<b>98.46</b>	<b>97.92</b>

539  
540

<b>14259 -85 (10-20µm)</b>									
	<b>Plag</b>	<b>Ilm</b>	<b>Olivine</b>	<b>Vol Gls.</b>	<b>Agglut. Gls.</b>	<b>Opx</b>	<b>Pig</b>	<b>Mg-Cpx</b>	<b>Fe-Cpx</b>
<b>SiO<sub>2</sub></b>	45.8	0.08	36.8	72.8	45.8 (31)	52.4	50.9	50.2	46.8
<b>TiO<sub>2</sub></b>	<0.04	52.4	0.05	0.45	1.64 (135)	0.90	0.77	0.92	0.99
<b>Al<sub>2</sub>O<sub>3</sub></b>	33.5	0.11	0.05	11.8	18.7 (57)	1.02	1.11	2.68	1.21
<b>Cr<sub>2</sub>O<sub>3</sub></b>	<0.04	0.42	<0.04	<0.04	0.16 (11)	0.27	0.32	0.73	0.18
<b>MgO</b>	0.05	3.63	33.3	0.09	8.33 (291)	23.5	18.4	15.4	5.81
<b>CaO</b>	17.4	0.16	0.16	1.24	11.8 (24)	1.93	4.83	14.4	12.2
<b>FeO</b>	0.10	39.6	27.7	2.16	9.81 (445)	17.7	21.1	13.6	29.5
<b>Na<sub>2</sub>O</b>	1.34	<0.04	<0.04	0.73	0.55 (40)	<0.04	<0.04	0.07	0.05
<b>K<sub>2</sub>O</b>	0.10	<0.04	<0.04	7.49	0.36 (39)	<0.04	<0.04	<0.04	<0.04
<b>Total</b>	<b>98.29</b>	<b>96.40</b>	<b>98.06</b>	<b>96.76</b>	<b>97.09</b>	<b>97.72</b>	<b>97.43</b>	<b>98.00</b>	<b>96.74</b>

541  
542

543  
544  
545  
546  
547

Table 5. Cont.

<b>61221 -9.2 (20-45µm)</b>									
	<b>Plag</b>	<b>Ilm</b>	<b>Olivine</b>	<b>Vol Gls.</b>	<b>Agglut. Gls.</b>	<b>Opx</b>	<b>Pig</b>	<b>Mg-Cpx</b>	<b>Fe-Cpx</b>
<b>SiO<sub>2</sub></b>	44.2	<0.04	37.7	46.4	45.1 (31)	53.0	51.6	50.8	45.0
<b>TiO<sub>2</sub></b>	<0.04	52.9	0.08	0.91	1.12 (185)	0.61	0.78	1.37	0.78
<b>Al<sub>2</sub>O<sub>3</sub></b>	35.3	0.18	0.15	1.10	24.2 (80)	1.06	1.22	1.99	0.95
<b>Cr<sub>2</sub>O<sub>3</sub></b>	<0.04	0.47	<0.04	<0.04	0.09 (13)	0.29	0.27	0.52	<0.04
<b>MgO</b>	<0.04	2.88	36.8	0.68	6.57 (485)	24.4	19.6	14.8	0.68
<b>CaO</b>	19.0	0.09	0.11	18.9	14.3 (35)	1.56	4.78	18.1	7.69
<b>FeO</b>	0.07	41.1	24.5	30.1	6.24 (557)	18.0	20.4	11.4	42.4
<b>Na<sub>2</sub>O</b>	0.56	<0.04	<0.04	0.14	0.54 (42)	<0.04	0.05	0.09	<0.04
<b>K<sub>2</sub>O</b>	<0.04	<0.04	<0.04	<0.04	0.16 (29)	<0.04	<0.04	<0.04	<0.04
<b>Total</b>	<b>99.13</b>	<b>97.62</b>	<b>99.34</b>	<b>98.23</b>	<b>98.30</b>	<b>98.92</b>	<b>98.70</b>	<b>99.07</b>	<b>97.50</b>

548  
549

<b>61221 -9.2 (10-20µm)</b>									
	<b>Plag</b>	<b>Ilm</b>	<b>Olivine</b>	<b>Vol Gls.</b>	<b>Agglut. Gls.</b>	<b>Opx</b>	<b>Pig</b>	<b>Mg-Cpx</b>	<b>Fe-Cpx</b>
<b>SiO<sub>2</sub></b>	44.1	0.08	38.0	65.9	45.3 (41)	53.3	51.9	51.0	48.6
<b>TiO<sub>2</sub></b>	<0.04	51.8	0.07	1.16	1.00 (170)	0.60	0.68	1.01	0.89
<b>Al<sub>2</sub>O<sub>3</sub></b>	34.9	0.10	0.08	12.1	23.1 (77)	0.95	1.16	1.48	1.11
<b>Cr<sub>2</sub>O<sub>3</sub></b>	<0.04	0.44	0.05	0.08	0.13 (15)	0.34	0.36	0.42	0.14
<b>MgO</b>	0.07	2.57	37.0	1.58	7.37 (484)	24.8	20.4	14.6	8.37
<b>CaO</b>	19.1	0.42	0.19	2.69	13.9 (36)	1.65	4.01	18.7	14.3
<b>FeO</b>	0.16	41.9	24.0	4.66	6.98 (545)	17.64	20.4	11.4	24.8
<b>Na<sub>2</sub>O</b>	0.58	<0.04	<0.04	1.42	0.43 (34)	<0.04	<0.04	0.07	0.07
<b>K<sub>2</sub>O</b>	0.04	0.05	<0.04	6.37	0.14 (26)	<0.04	<0.04	<0.04	<0.04
<b>Total</b>	<b>98.95</b>	<b>97.36</b>	<b>99.39</b>	<b>95.96</b>	<b>98.37</b>	<b>99.28</b>	<b>98.91</b>	<b>98.68</b>	<b>98.28</b>

550  
551

552  
553  
554  
555  
556

Table 5. Cont.

<b>67461 -25 (20-45µm)</b>									
	<b>Plag</b>	<b>Ilm</b>	<b>Olivine</b>	<b>Vol Gls.</b>	<b>Agglut. Gls.</b>	<b>Opx</b>	<b>Pig</b>	<b>Mg-Cpx</b>	<b>Fe-Cpx</b>
<b>SiO<sub>2</sub></b>	44.0	0.04	36.1	72.7	43.9 (43)	53.3	52.1	50.5	46.4
<b>TiO<sub>2</sub></b>	<0.04	52.4	0.06	0.35	0.53 (55)	0.56	0.51	1.06	0.82
<b>Al<sub>2</sub>O<sub>3</sub></b>	35.0	0.07	<0.04	9.74	24.6 (79)	0.99	1.27	1.53	0.72
<b>Cr<sub>2</sub>O<sub>3</sub></b>	<0.04	0.20	0.04	<0.04	0.15 (48)	0.38	0.42	0.56	0.05
<b>MgO</b>	0.06	2.33	30.9	0.12	7.47 (547)	25.4	22.3	14.3	4.01
<b>CaO</b>	19.2	0.22	0.11	0.47	14.6 (37)	1.52	4.51	19.0	15.7
<b>FeO</b>	0.15	42.4	31.9	5.26	6.48 (481)	16.9	17.3	11.5	28.0
<b>Na<sub>2</sub>O</b>	0.54	<0.04	<0.04	0.11	0.40 (24)	<0.04	<0.04	0.06	0.04
<b>K<sub>2</sub>O</b>	<0.04	<0.04	<0.04	7.11	0.08 (17)	<0.04	<0.04	<0.04	-----
<b>Total</b>	<b>98.95</b>	<b>97.66</b>	<b>99.11</b>	<b>95.86</b>	<b>98.26</b>	<b>99.05</b>	<b>98.41</b>	<b>98.51</b>	<b>95.74</b>

557  
558  
559

<b>67461 -25 (10-20µm)</b>									
	<b>Plag</b>	<b>Ilm</b>	<b>Olivine</b>	<b>Vol Gls.</b>	<b>Agglut. Gls.</b>	<b>Opx</b>	<b>Pig</b>	<b>Mg-Cpx</b>	<b>Fe-Cpx</b>
<b>SiO<sub>2</sub></b>	44.3	0.04	36.6	73.4	43.7 (48)	52.7	51.9	50.8	47.5
<b>TiO<sub>2</sub></b>	<0.04	52.7	0.05	0.35	0.55 (35)	0.51	0.55	1.01	0.83
<b>Al<sub>2</sub>O<sub>3</sub></b>	34.6	0.09	<0.04	9.92	24.9 (67)	0.79	1.36	1.43	0.75
<b>Cr<sub>2</sub>O<sub>3</sub></b>	<0.04	0.22	0.04	<0.04	0.15 (23)	0.43	0.43	0.53	0.05
<b>MgO</b>	0.07	2.38	31.0	0.10	7.28 (497)	25.6	22.9	14.8	4.21
<b>CaO</b>	19.3	0.23	0.11	0.42	13.9 (47)	1.15	4.54	18.6	15.8
<b>FeO</b>	0.18	42.7	31.7	5.12	6.63 (453)	16.7	17.0	11.4	29.5
<b>Na<sub>2</sub>O</b>	0.55	<0.04	<0.04	0.13	0.36 (19)	<0.04	<0.04	0.05	0.04
<b>K<sub>2</sub>O</b>	<0.04	<0.04	<0.04	7.81	0.07 (11)	<0.04	<0.04	<0.04	-----
<b>Total</b>	<b>99.00</b>	<b>98.36</b>	<b>99.50</b>	<b>97.25</b>	<b>97.54</b>	<b>97.88</b>	<b>98.68</b>	<b>98.62</b>	<b>98.64</b>

560  
561

562  
563  
564  
565  
566

**Table 5. Cont.**

<b>67481 -31 (20-45µm)</b>									
	<b>Plag</b>	<b>Ilm</b>	<b>Olivine</b>	<b>Vol Gls.</b>	<b>Agglut. Gls.</b>	<b>Opx</b>	<b>Pig</b>	<b>Mg-Cpx</b>	<b>Fe-Cpx</b>
<b>SiO<sub>2</sub></b>	44.2	0.09	36.9	68.9	44.3 (36)	52.6	52.8	51.1	47.6
<b>TiO<sub>2</sub></b>	<0.04	53.1	0.08	0.27	0.76 (301)	0.53	0.59	1.14	1.33
<b>Al<sub>2</sub>O<sub>3</sub></b>	35.0	<0.04	0.08	15.3	25.6 (69)	0.85	0.85	1.51	0.79
<b>Cr<sub>2</sub>O<sub>3</sub></b>	<0.04	0.23	0.06	<0.04	0.14 (15)	0.33	0.32	0.55	0.17
<b>MgO</b>	0.06	2.81	33.1	0.10	6.53 (502)	23.3	22.2	14.3	4.49
<b>CaO</b>	19.1	0.10	0.07	1.31	15.1 (35)	1.40	4.42	18.5	17.1
<b>FeO</b>	0.06	42.6	29.3	0.09	5.59 (490)	19.9	18.0	11.9	27.1
<b>Na<sub>2</sub>O</b>	0.56	0.04	<0.04	0.32	0.43 (22)	<0.04	<0.04	0.09	0.11
<b>K<sub>2</sub>O</b>	0.06	0.04	<0.04	10.7	0.08 (10)	<0.04	<0.04	<0.04	<0.04
<b>Total</b>	<b>99.04</b>	<b>99.01</b>	<b>99.59</b>	<b>96.99</b>	<b>98.51</b>	<b>98.91</b>	<b>99.18</b>	<b>99.09</b>	<b>98.69</b>

567  
568

<b>67481-31 (10-20µm)</b>									
	<b>Plag</b>	<b>Ilm</b>	<b>Olivine</b>	<b>Vol Gls.</b>	<b>Agglut. Gls.</b>	<b>Opx</b>	<b>Pig</b>	<b>Mg-Cpx</b>	<b>Fe-Cpx</b>
<b>SiO<sub>2</sub></b>	44.6	0.07	37.1	70.5	44.5 (38)	53.1	53.1	51.7	48.4
<b>TiO<sub>2</sub></b>	<0.04	52.8	0.07	0.37	0.85 (138)	0.59	0.61	0.94	0.90
<b>Al<sub>2</sub>O<sub>3</sub></b>	34.6	<0.04	<0.04	14.3	24.6 (69)	0.79	0.96	1.30	0.70
<b>Cr<sub>2</sub>O<sub>3</sub></b>	<0.04	0.31	0.07	<0.04	0.13 (13)	0.34	0.31	0.44	0.05
<b>MgO</b>	0.08	2.58	33.9	<0.04	7.03 (446)	24.3	22.0	14.9	5.04
<b>CaO</b>	18.9	0.25	0.14	1.71	14.7 (32)	1.69	3.96	19.3	16.8
<b>FeO</b>	0.15	42.0	28.2	0.43	6.20 (468)	18.3	18.8	10.8	26.6
<b>Na<sub>2</sub>O</b>	0.65	<0.04	<0.04	0.67	0.44 (54)	<0.04	<0.04	0.05	0.06
<b>K<sub>2</sub>O</b>	0.06	<0.04	<0.04	9.11	0.18 (73)	<0.04	<0.04	<0.04	<0.04
<b>Total</b>	<b>99.04</b>	<b>98.01</b>	<b>99.48</b>	<b>97.09</b>	<b>98.64</b>	<b>99.11</b>	<b>99.74</b>	<b>99.43</b>	<b>98.55</b>

569  
570

571  
572  
573  
574  
575

**Table 5. Cont.**

<b>61141 -56 (20-45µm)</b>									
	<b>Plag</b>	<b>Ilm</b>	<b>Olivine</b>	<b>Vol Gls.</b>	<b>Agglut. Gls.</b>	<b>Opx</b>	<b>Pig</b>	<b>Mg-Cpx</b>	<b>Fe-Cpx</b>
<b>SiO<sub>2</sub></b>	44.3	<0.04	37.7	71.5	44.2 (41)	52.8	52.2	51.4	45.2
<b>TiO<sub>2</sub></b>	<0.04	53.4	0.06	0.35	1.05 (169)	0.66	0.61	0.85	0.89
<b>Al<sub>2</sub>O<sub>3</sub></b>	34.9	0.06	0.06	14.4	23.5 (83)	0.86	0.97	1.29	0.87
<b>Cr<sub>2</sub>O<sub>3</sub></b>	<0.04	0.38	0.07	<0.04	0.16 (16)	0.33	0.33	0.40	0.08
<b>MgO</b>	0.04	3.78	37.7	0.15	7.52 (516)	24.6	21.3	15.1	0.69
<b>CaO</b>	18.9	0.13	0.11	1.55	14.3 (37)	1.61	4.62	20.0	10.4
<b>FeO</b>	0.10	40.8	23.5	0.68	7.17 (583)	18.0	18.8	9.57	39.8
<b>Na<sub>2</sub>O</b>	0.70	<0.04	<0.04	0.86	0.40 (28)	<0.04	<0.04	0.07	<0.04
<b>K<sub>2</sub>O</b>	0.05	<0.04	<0.04	7.70	0.11 (25)	<0.04	<0.04	<0.04	<0.04
<b>Total</b>	<b>98.99</b>	<b>98.65</b>	<b>99.20</b>	<b>97.19</b>	<b>98.47</b>	<b>98.86</b>	<b>98.83</b>	<b>98.68</b>	<b>97.93</b>

576  
577

<b>61141 -56 (10-20µm)</b>									
	<b>Plag</b>	<b>Ilm</b>	<b>Olivine</b>	<b>Vol Gls.</b>	<b>Agglut. Gls.</b>	<b>Opx</b>	<b>Pig</b>	<b>Mg-Cpx</b>	<b>Fe-Cpx</b>
<b>SiO<sub>2</sub></b>	44.4	0.07	37.8	74.2	44.5 (41)	53.6	52.6	51.0	44.9
<b>TiO<sub>2</sub></b>	0.05	52.9	0.10	0.17	0.88 (129)	0.72	0.80	1.15	0.84
<b>Al<sub>2</sub>O<sub>3</sub></b>	34.6	<0.04	<0.04	11.7	23.9 (72)	1.05	1.05	1.39	0.97
<b>Cr<sub>2</sub>O<sub>3</sub></b>	<0.04	0.44	0.06	<0.04	0.14 (12)	0.44	0.43	0.38	0.09
<b>MgO</b>	0.07	2.96	37.3	0.42	7.60 (448)	25.8	22.5	14.3	1.03
<b>CaO</b>	19.0	0.21	0.13	0.64	14.5 (33)	1.75	4.51	19.1	10.7
<b>FeO</b>	0.17	41.7	24.2	1.63	6.75 (445)	16.1	17.2	11.5	39.9
<b>Na<sub>2</sub>O</b>	0.68	<0.04	<0.04	1.32	0.42 (38)	<0.04	<0.04	0.09	<0.04
<b>K<sub>2</sub>O</b>	0.07	<0.04	<0.04	8.40	0.14 (26)	<0.04	<0.04	<0.04	<0.04
<b>Total</b>	<b>99.04</b>	<b>98.28</b>	<b>99.59</b>	<b>98.48</b>	<b>98.75</b>	<b>99.46</b>	<b>99.09</b>	<b>98.91</b>	<b>98.43</b>

578  
579

580  
581  
582  
583  
584

**Table 5. Cont.**

<b>64801 -82 (20-45µm)</b>									
	<b>Plag</b>	<b>Ilm</b>	<b>Olivine</b>	<b>Vol Gls.</b>	<b>Agglut. Gls.</b>	<b>Opx</b>	<b>Pig</b>	<b>Mg-Cpx</b>	<b>Fe-Cpx</b>
<b>SiO<sub>2</sub></b>	44.1	0.06	37.7	73.5	45.5 (38)	53.3	51.4	50.8	48.6
<b>TiO<sub>2</sub></b>	<0.04	53.3	0.07	0.39	1.02 (143)	0.78	0.73	1.34	0.36
<b>Al<sub>2</sub>O<sub>3</sub></b>	34.7	0.15	0.06	12.1	22.7 (78)	1.17	1.12	1.84	0.59
<b>Cr<sub>2</sub>O<sub>3</sub></b>	<0.04	0.39	0.08	<0.04	0.13 (12)	0.41	0.36	0.56	0.24
<b>MgO</b>	<0.04	4.01	37.1	<0.04	6.97 (503)	26.1	19.6	15.3	5.40
<b>CaO</b>	19.3	0.22	0.15	0.93	13.9 (36)	1.84	4.75	18.5	19.3
<b>FeO</b>	0.07	40.4	24.1	1.64	7.02 (502)	15.5	20.6	10.4	23.9
<b>Na<sub>2</sub>O</b>	0.47	<0.04	<0.04	0.93	0.42 (35)	<0.04	<0.04	0.09	0.08
<b>K<sub>2</sub>O</b>	<0.04	0.04	<0.04	7.93	0.21 (58)	<0.04	<0.04	<0.04	<0.04
<b>Total</b>	<b>98.64</b>	<b>98.57</b>	<b>99.26</b>	<b>97.42</b>	<b>97.97</b>	<b>99.10</b>	<b>98.56</b>	<b>98.83</b>	<b>98.47</b>

585  
586

<b>64801 -82 (10-20µm)</b>									
	<b>Plag</b>	<b>Ilm</b>	<b>Olivine</b>	<b>Vol Gls.</b>	<b>Agglut. Gls.</b>	<b>Opx</b>	<b>Pig</b>	<b>Mg-Cpx</b>	<b>Fe-Cpx</b>
<b>SiO<sub>2</sub></b>	43.9	0.04	37.7	70.8	44.8 (31)	53.5	52.4	50.6	48.4
<b>TiO<sub>2</sub></b>	<0.04	52.6	0.08	0.62	0.76 (98)	0.66	0.78	1.74	0.83
<b>Al<sub>2</sub>O<sub>3</sub></b>	34.7	0.06	<0.04	12.7	23.8 (71)	1.18	1.15	2.14	1.20
<b>Cr<sub>2</sub>O<sub>3</sub></b>	<0.04	0.56	0.08	<0.04	0.13 (13)	0.41	0.38	0.54	0.08
<b>MgO</b>	0.07	2.77	37.4	0.52	7.24 (460)	26.4	22.6	15.9	6.58
<b>CaO</b>	19.3	0.32	0.18	2.02	14.3 (34)	1.74	4.48	17.7	15.9
<b>FeO</b>	0.15	41.7	23.7	3.03	6.41 (446)	15.1	17.0	10.2	25.4
<b>Na<sub>2</sub>O</b>	0.51	<0.04	<0.04	0.72	0.42 (47)	<0.04	<0.04	0.09	0.08
<b>K<sub>2</sub>O</b>	<0.04	<0.04	<0.04	5.81	0.19 (46)	<0.04	<0.04	<0.04	<0.04
<b>Total</b>	<b>98.63</b>	<b>98.05</b>	<b>99.14</b>	<b>96.22</b>	<b>98.09</b>	<b>98.99</b>	<b>98.79</b>	<b>98.91</b>	<b>98.47</b>

587  
588



589  
590  
591  
592  
593

**Table 5. Cont.**

<b>62231 -91 (20-45µm)</b>									
	<b>Plag</b>	<b>Ilm</b>	<b>Olivine</b>	<b>Vol Gls.</b>	<b>Agglut. Gls.</b>	<b>Opx</b>	<b>Pig</b>	<b>Mg-Cpx</b>	<b>Fe-Cpx</b>
<b>SiO<sub>2</sub></b>	43.7	0.07	37.7	71.6	44.5 (39)	53.1	52.1	50.8	47.8
<b>TiO<sub>2</sub></b>	<0.04	52.6	0.08	0.39	0.92 (111)	0.68	0.60	1.10	1.39
<b>Al<sub>2</sub>O<sub>3</sub></b>	35.0	0.10	<0.04	13.7	23.0 (80)	0.89	0.98	1.39	1.69
<b>Cr<sub>2</sub>O<sub>3</sub></b>	0.05	0.39	0.14	0.07	0.21 (19)	0.42	0.44	0.49	0.17
<b>MgO</b>	0.07	2.83	37.1	0.56	7.69 (546)	25.2	20.9	14.5	6.53
<b>CaO</b>	19.3	0.22	0.13	1.24	14.1 (36)	1.71	4.63	19.0	13.3
<b>FeO</b>	0.15	42.1	24.0	0.71	7.26 (490)	16.8	19.1	11.2	27.9
<b>Na<sub>2</sub>O</b>	0.50	<0.04	<0.04	1.19	0.41 (31)	<0.04	<0.04	0.07	0.05
<b>K<sub>2</sub>O</b>	0.04	0.04	<0.04	7.51	0.15 (22)	<0.04	<0.04	<0.04	<0.04
<b>Total</b>	<b>98.81</b>	<b>98.31</b>	<b>99.15</b>	<b>96.97</b>	<b>98.20</b>	<b>98.80</b>	<b>98.75</b>	<b>98.55</b>	<b>98.83</b>

594  
595

<b>62231 -91 (10-20µm)</b>									
	<b>Plag</b>	<b>Ilm</b>	<b>Olivine</b>	<b>Vol Gls.</b>	<b>Agglut. Gls.</b>	<b>Opx</b>	<b>Pig</b>	<b>Mg-Cpx</b>	<b>Fe-Cpx</b>
<b>SiO<sub>2</sub></b>	44.2	0.08	37.4	68.2	44.4 (37)	53.3	52.6	51.3	47.6
<b>TiO<sub>2</sub></b>	<0.04	52.7	0.09	0.20	0.91 (132)	0.59	0.74	1.17	1.36
<b>Al<sub>2</sub>O<sub>3</sub></b>	34.8	0.06	<0.04	15.4	23.0 (76)	0.98	1.09	1.55	1.58
<b>Cr<sub>2</sub>O<sub>3</sub></b>	<0.04	0.51	0.08	<0.04	0.18 (14)	0.39	0.41	0.46	0.13
<b>MgO</b>	0.06	3.24	35.2	0.16	7.66 (464)	24.2	21.9	14.8	6.09
<b>CaO</b>	19.2	0.33	0.17	1.52	14.2 (35)	1.69	4.43	18.2	13.8
<b>FeO</b>	0.11	41.2	26.5	1.37	7.34 (527)	18.0	18.1	11.6	28.0
<b>Na<sub>2</sub>O</b>	0.53	<0.04	<0.04	1.11	0.45 (53)	<0.04	<0.04	0.08	0.04
<b>K<sub>2</sub>O</b>	0.05	<0.04	<0.04	9.40	0.14 (29)	<0.04	<0.04	<0.04	<0.04
<b>Total</b>	<b>98.95</b>	<b>98.12</b>	<b>99.44</b>	<b>97.36</b>	<b>98.29</b>	<b>99.15</b>	<b>99.27</b>	<b>99.16</b>	<b>98.60</b>

596  
597

Figure 1. Modal analyses of phases in the fine fractions of highland soils. These data are modified after those in a LPSC abstract [Taylor et al., 2003].

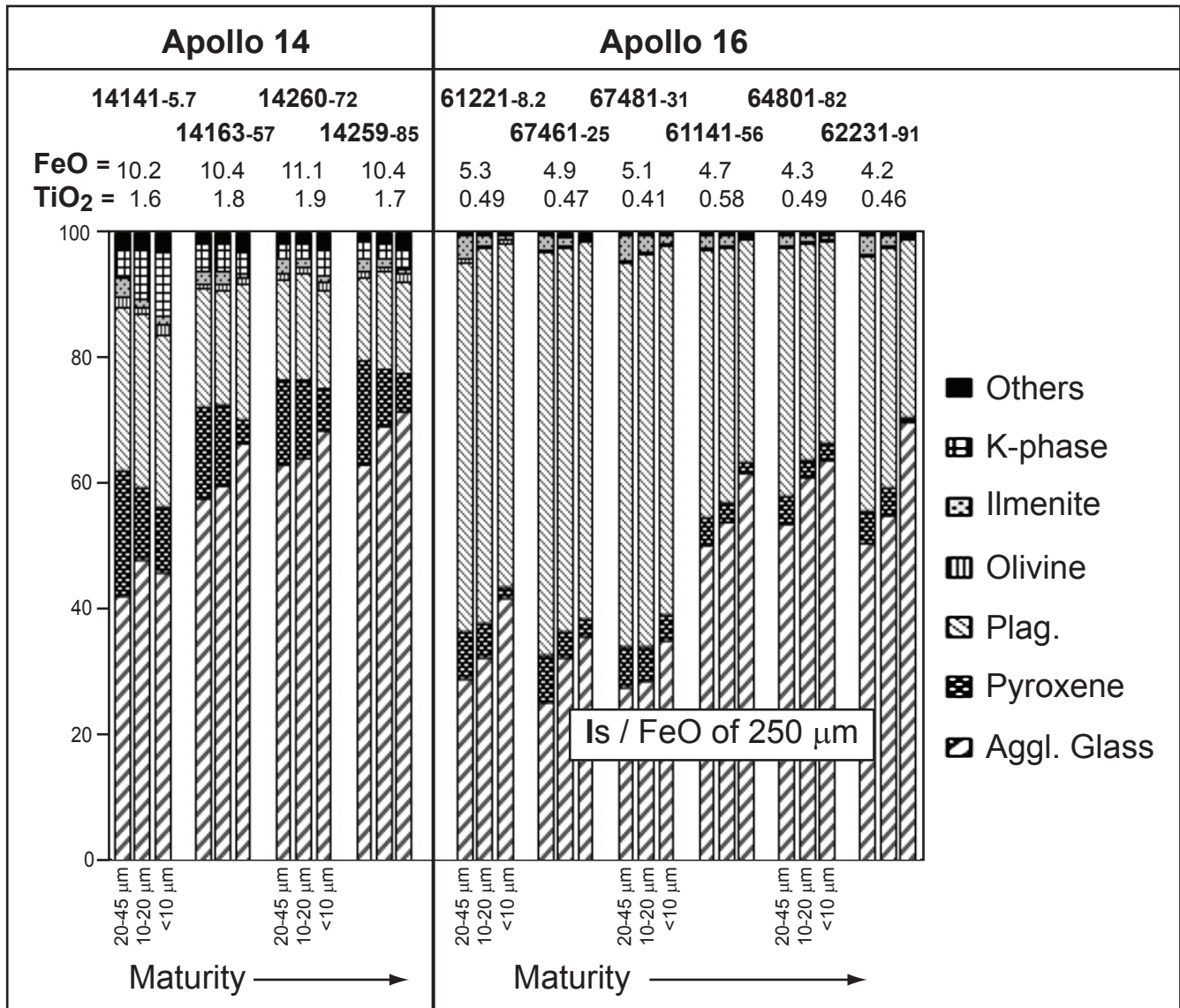


Figure 2. Comparisons of oxide components of the bulk chemistry of the fine fractions of high-land soils, in addition to their  $I_s/FeO$  values.

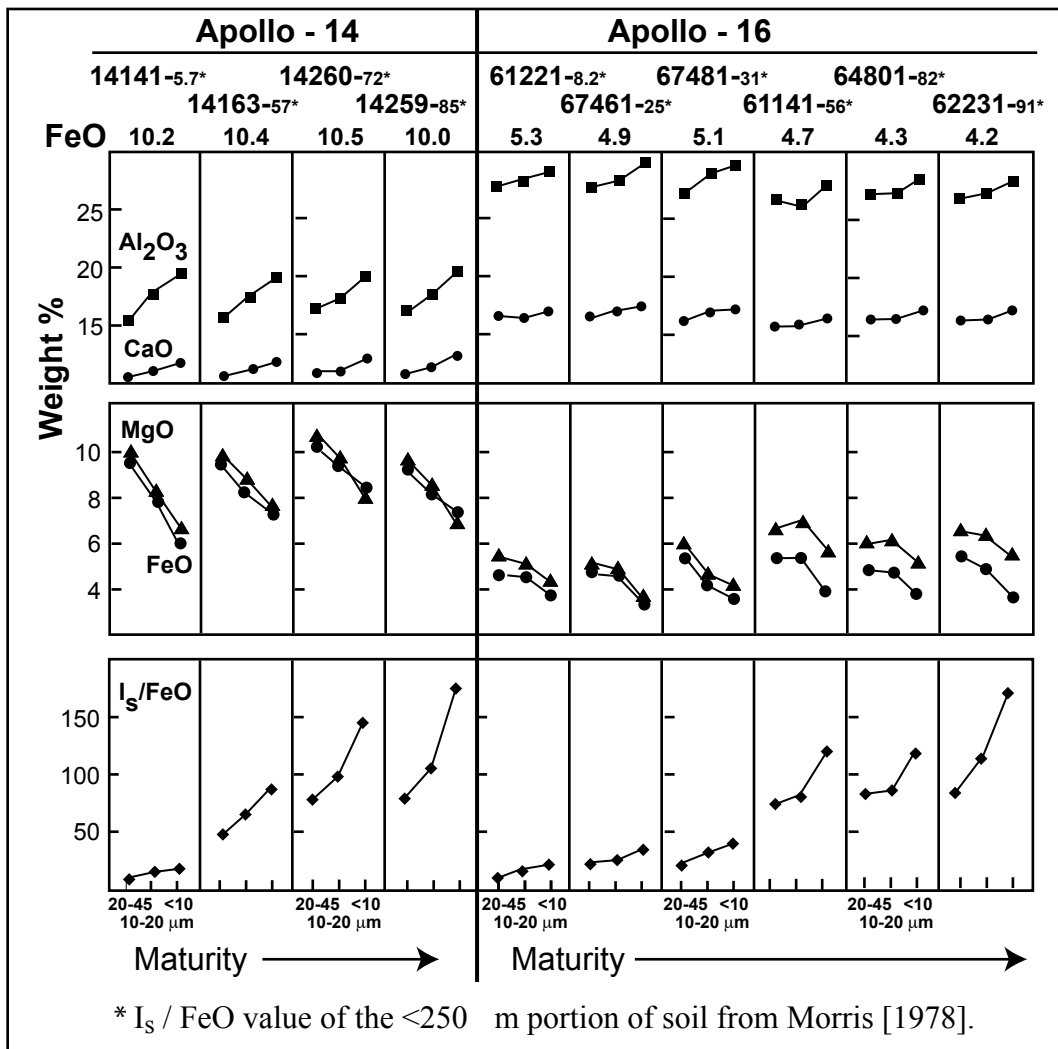


Figure 3. Comparison of chemistry of the agglutinitic glass with the bulk chemistry of the three soil size fractions for Apollo 16 highland soils. Modified from LPSC abstract [Taylor et al., 2003].

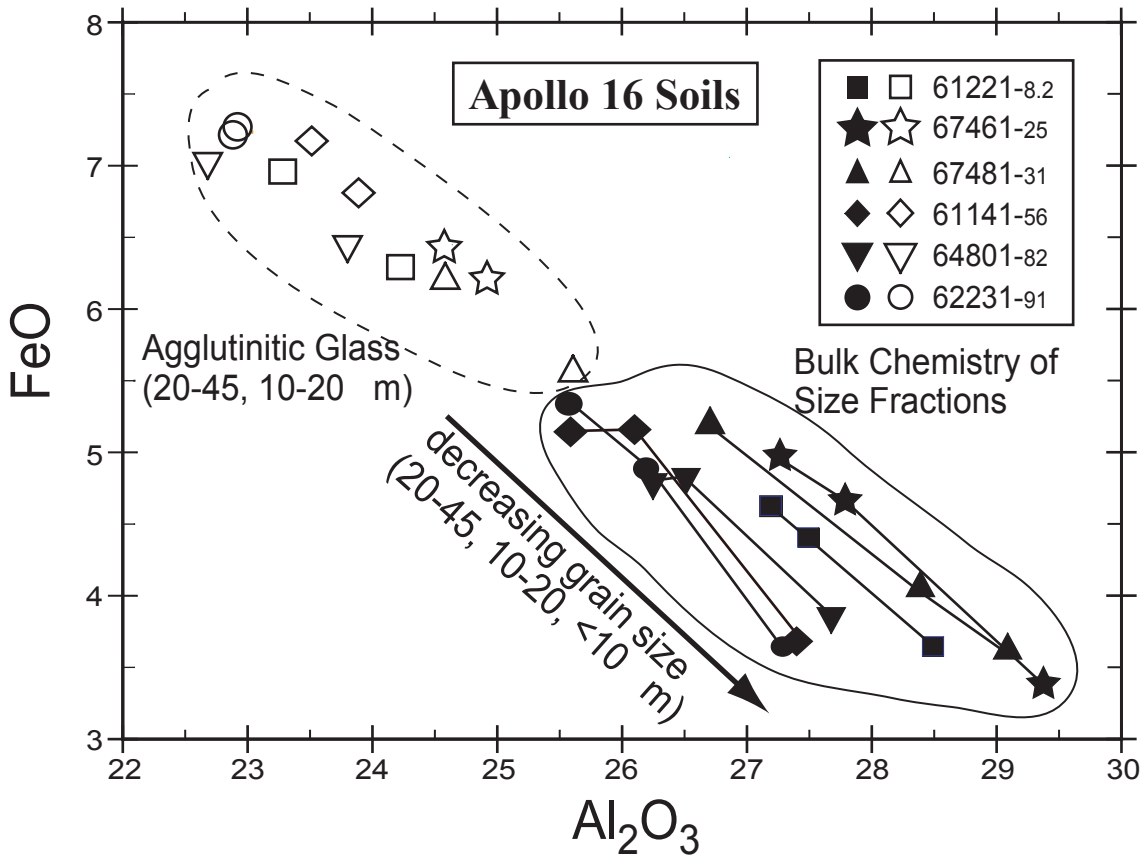




Figure 5. Bi-directional reflectance spectra of LSCC highland soils. Data for 64801 are from Pieters and Taylor [2003a].

